

This is the accepted manuscript version of the contribution published as:

Prata Rabelo, U., Dietrich, J., Cunha Costa, A., Simshäuser, M.N., Scholz, F.E., **Nguyen, V.T.**, Lima Neto, I.E. (2021):
Representing a dense network of ponds and reservoirs in a semi-distributed dryland catchment model
J. Hydrol. **603, Part C** , art. 127103

The publisher's version is available at:

<http://dx.doi.org/10.1016/j.jhydrol.2021.127103>

1 Representing a dense network of ponds and reservoirs in a 2 semi-distributed dryland catchment model

3 Udinart Prata Rabelo^{a,*}, Jörg Dietrich^b, Alexandre Cunha Costa^c, Max Nino Simshäuser^b, Fernanda
4 Elise Scholz^b, Tam V. Nguyen^d, Iran Eduardo Lima Neto^a.

5 ^a Department of Hydraulic Engineering and Environment, Federal University of Ceará, Campus do
6 Pici, 60.451-970, Fortaleza, Brazil

7 ^b Institute of Hydrology and Water Resources Management, Leibniz Universität Hannover, Appelstr.
8 9A, 30419 Hannover, Germany

9 ^c Institute of Engineering and Sustainable Development, University of International Integration of the
10 Afro-Brazilian Lusophony, Campus das Auroras, Rua José Franco de Oliveira, s/n, 62.790-970,
11 Redenção, Brazil

12 ^d Helmholtz Centre for Environmental Research - UFZ, Department of Hydrogeology, Permoserstr.
13 15, 04318 Leipzig, Germany

14

15 Abstract

16 The mismatch between natural water availability and demand in dryland regions is overcome
17 by reservoirs of different sizes with the purpose of storing water. The increase in population in
18 dryland regions and the consequent growth in water demand expanded the construction of small
19 reservoirs, generating in these regions a dense network of reservoirs, which increases the
20 complexity of modeling these hydrological systems. For dryland watersheds modeling with
21 daily time-step, the horizontal connectivity of the reservoir network needs careful
22 representation in order to achieve acceptable model performance, including cumulative effects
23 of reservoirs. However, the horizontal connectivity of reservoir networks is often less
24 investigated in large-scale catchment models. This work presents an innovative way of
25 implementing the dense-reservoir network into the widely used eco-hydrological model Soil

*Corresponding author

Email address: udinart@gmail.com (Udinart Prata Rabelo)

26 and Water Assessment Tool (SWAT), with detailed representation of large and small
27 reservoirs, and an extensive analysis about the cumulative impact of small reservoirs on the
28 horizontal hydrological connectivity for large-scale dryland catchments. A two-fold cross-
29 validation was used against streamflow at a catchment outlet and against in-catchment reservoir
30 water levels. The model daily performance was acceptable despite the input data uncertainty,
31 with good reliability for peak flow in wet years, for nonflow periods and for the rising limb of
32 the hydrograph. The efforts in the parameterization of reservoirs and aggregation of ponds
33 allowed a better analysis of the hydrological processes and their impacts in the catchment. The
34 results showed that small reservoirs decreased the streamflow, but had a low impact on
35 catchment retention and water losses, with 2% of water retention in wet years. However, the
36 water retention reached 9% in dry years, which may worsen periods of water scarcity in the
37 large reservoirs. The spatial representation of small reservoirs for a high-density network in the
38 SWAT model and the results of the cumulative impact of small reservoirs may be relevant for
39 a better understanding of hydrology in dryland catchments, and can be applied to catchments
40 in similar climatic and socio-economic environments.

41 **Keywords:** SWAT, dryland hydrology, pond, reservoir, hydrological connectivity

42

43 **1 Introduction**

44 Dryland environments are home to the world's water poorest populations and, during recent
45 decades, have been subjected to increases in population, partial rise in living standards,
46 development of irrigated agriculture, and new activities – especially tourism – that have
47 drastically changed water and land use. These populations are vulnerable to the adverse
48 consequences of environmental changes and in need of regional hydrological studies for better
49 water resources management and water-scarcity risk reduction (Gutiérrez et al., 2014;
50 AghaKouchak et al., 2015; Mallakpour et al., 2018; Samimi et al., 2020; Yao et al., 2020). To

51 overcome the mismatch between natural water availability and demand, dams of different sizes
52 have been built with the purpose of storing large amounts of water during the wet season, which
53 may then be used during the dry season and dry years (Simmers, 2003; Mamede et al., 2012;
54 Mady et al., 2020).

55 The increase in population in dryland regions and the consequent growth in water demand
56 for human activities expanded the number of large, medium and small dams distributed along
57 the catchments (Mady et al., 2020; Samimi et al., 2020). The federal and state governments of
58 dryland regions have promoted the construction of large reservoirs, which mainly serve to
59 provide for the water demand of industries, urban regions and large-scale irrigation agriculture
60 (Araújo and Medeiros, 2013). Additionally, small-scale reservoirs have been used for a long
61 time, mainly in dryland regions, as a complement to meet the water demand of small
62 municipalities, rural communities and farmers. The small-sized and seasonal freshwater system
63 play an important role in reducing inequalities for rural populations, providing sustainable
64 development for rural communities and farmers. Due to their reduced cost and availability of
65 many favourable locations, the number of small reservoirs has increased in recent decades
66 (Araújo and Medeiros, 2013; Berhane et al., 2016; Yaeger et al., 2017; Habets et al., 2018).

67 The spatial density of small reservoirs varies across different regions, with catchments in
68 India with 4.2 reservoirs per km², Northeastern Brazil with 0.2 reservoir per km² and Australia
69 with values between 0.15 to 6.1 reservoirs per km², for example. The advances of remote
70 sensing techniques in obtaining important information from satellite images have allowed a
71 better identification of the dimensions and uses of small reservoirs and assessing their global
72 distribution (Lima Neto et al., 2011; Carluer et al., 2016; Mady et al, 2020; Paredes-Beltran et
73 al., 2021). The small reservoirs (medium to micro-dams) are usually built disregarding the
74 potential impact on the water availability of downstream communities. This has led to the
75 generation of a chaotic system, which is referred to as a *high-density reservoir network* (Lima

76 Neto et al., 2011; Mamede et al., 2012; Abouabdillah et al., 2014). On the one hand, such a
77 reservoir network ensures a more equally distributed use of the water resources among the
78 population of the river basin, as it reduces the concentration of water in large downstream
79 reservoirs and enhances an even spatial distribution (Mamede et al., 2012; Fowe et al., 2015;
80 Zhang et al., 2016). This has also positive effects such as decreasing sedimentation in the large
81 strategic reservoirs (Lima Neto et al., 2011; Berg et al., 2015; Mamede et al., 2018), decreasing
82 soil erosion (Abouabdillah et al., 2014) and decreasing the energy demand for pumping
83 (Nascimento et al., 2019). On the other hand, as the smaller dams are also designed to maximize
84 storage and the flow in tributaries is rare, the spilling frequency of the reservoirs is low,
85 increasing hydrological discontinuity (Araújo and Medeiros, 2013; Abouabdillah et al., 2014;
86 Peter et al., 2014).

87 The cumulative impact of the small reservoirs on downstream water availability are not
88 simple to estimate because they are not necessarily the sum of individual effects of each small
89 reservoir. These reservoirs may be inter-dependent and the cumulative effect can be greater or
90 less than the sum of the individual effects, depending on their dimensions, uses and locations.
91 (Habets et al., 2018). However, there is evidence that the cumulative impact of the small
92 reservoirs can be considerable, as the inflow to the large downstream reservoirs is reduced
93 (Malveira et al., 2012; Araújo and Medeiros, 2013; Fowler et al., 2016). Some modeling
94 approaches have been developed to assess the effects of small reservoirs in a basin. Most of
95 them reported a decrease on the annual stream discharge, with a wide range from 0.2% to 36%
96 and decreases in low flow and peak flow (Neal et al., 2002; Schreider et al., 2002; Nathan et
97 al., 2005; Callow and Smettem, 2009; Hughes and Mantel, 2010; Nathan and Lowe, 2012;
98 Fowe et al., 2015; Ayalew et al., 2017; Habets et al., 2018; Zhang et al., 2020).

99 Most of those models are, however, based on simple mass balance methods developed for
100 dryland environments. Thus, their application in a scenario of increase in the number of small

101 reservoirs should be done with caution, due to specific water use and hydraulic infrastructure
102 patterns. Moreover, despite the importance of the small reservoirs for local needs and their
103 impact on water availability at catchment scale, the small reservoirs have been neglected by
104 water authorities, providing little technical information about them (Fowe et al., 2015; Habets
105 et al., 2018). Reservoir data scarcity hampers, therefore, successful hydrological model
106 application to drylands and semi-arid environments with high-density reservoir networks,
107 which already face both poor monitoring of streamflow and extreme precipitation variation
108 from year to year. The lack of information on small reservoirs characteristics and the difficulty
109 to estimate cumulative impact is a challenge to assess and to model the hydrology in dryland
110 environments.

111 The incorporation of reservoirs in hydrological models was carried out using simplified
112 approaches in several other studies to assess their impact in streamflow. In WASA (Model of
113 Water Availability in Semi-arid Environments) the reservoirs are grouped into size classes
114 according to their storage capacity, with reservoirs of a smaller size class located upstream of
115 reservoirs of a higher size class, and arranged in a cascade system, with only reservoirs of the
116 largest size class regarded explicitly in the model in daily or hourly steps (Güntner, 2002;
117 Güntner et al., 2004; Medeiros et al., 2018). The TEDI (Tool for Estimating Dam Impacts)
118 model also uses as model input the dam size distribution, subdivided into classes, with
119 computations on a monthly basis. TEDI assumes that reservoirs are connected in parallel, and
120 the excess water spilling from each reservoir is directly routed to the outlet of the catchment,
121 disregarding the spatial arrangement of the single reservoirs. Subsequently, the CHEAT
122 (Complex Hydrological Evaluation of the Assumptions in TEDI) tool was developed by
123 Nathan et al. (2005) and included information on the location of the reservoirs on the river
124 network and the network topology, thus differentiating also between sequential and parallel
125 arrangement of single reservoirs (Nathan and Lowe, 2012; Fowler et al., 2016). However, the

126 horizontal connectivity of reservoir networks is often less investigated in large-scale catchment
127 models.

128 The eco-hydrological model SWAT (Soil and Water Assessment Tool, Arnold et al., 2012)
129 has been applied worldwide for the simulation of catchments, in particular where water
130 extractions and agricultural water management are of major relevance (e.g., Uniyal et al., 2019
131 with study areas in India, Chile, Vietnam and Germany). Various SWAT applications regarding
132 the hydrology of dryland areas in China, Mongolia, Azerbaijan, Pakistan, Tunisia, Algeria,
133 Mexico and Brazil have been published (Abouabdillah et al., 2014; Bressiani et al., 2015;
134 Ghoraba, 2015; Molina-Navarro et al., 2015; Luo et al., 2016; Siqueira et al., 2016; Sukhbaatar
135 et al., 2017; Sun et al., 2017; Zettam et al., 2017; Santos et al., 2018; Andaryani et al., 2019;
136 Andrade et al., 2019). Despite this, there are few examples of studies (e.g., Zhang et al., 2012;
137 Liu et al., 2014; Nguyen et al., 2017) that investigate the impacts of the combination of
138 reservoirs of different types and levels of operation on catchment runoff using SWAT. In fact,
139 approaches that mimic the effects of a large number of reservoirs in hydrological model
140 structures have rarely been published. To achieve acceptable model performance in dryland
141 watersheds for daily time steps modeling, the implementation of the reservoir network and its
142 horizontal connectivity is fundamental, with detailed representation of large and small
143 reservoirs, enabling a better analysis of their cumulative effects.

144 This paper investigates capabilities of the eco-hydrological catchment model SWAT to
145 represent dense networks of large and small reservoirs as common for many dryland regions,
146 as well as to gain in-depth understanding of hydrological processes and reservoir storage for
147 meso-scale dryland catchments. To accomplish this goal, a detailed approach for dense
148 networks of reservoirs is modeled in the eco-hydrological model SWAT, for daily time steps.
149 A new modeling and parameterization strategy of ponds and reservoirs is developed with
150 detailed representation, focusing on the horizontal hydrological connectivity and the

151 cumulative impact of small reservoirs, together with the parameterization of transmission
152 losses and flood routing based on a modified SWAT version (Nguyen et al., 2018), with a
153 corrected Muskingum subroutine suggested by the authors. The catchment in the SWAT model
154 is evaluated using streamflow and reservoir water level series by a two-fold cross-validation
155 approach. Moreover, a reservoir scenario approach is performed to assess the impact of the
156 large and small reservoirs on the streamflow and storage volume, including different
157 combinations of small reservoir dimensions. The present study not only improves the
158 understanding of the hydrology of dense reservoir networks but also proposes a modeling
159 approach that can be applied to water resources management in dryland catchments.

160

161 **2 Materials and methods**

162 ***2.1 Study area: catchment***

163 The region for application of the model is a dryland meso-scale catchment in Brazil. The
164 Conceição River (catchment area: 3,347 km²) is located in the state of Ceará in the Northeast
165 of Brazil (Figure 1). The discharge from the watershed outlet is monitored daily at the Malhada
166 gauging station. The Conceição River is a tributary of the Upper Jaguaribe (*Alto-Jaguaribe*)
167 River Basin (UJB), which is itself a sub-catchment of the Jaguaribe River watershed. The
168 Jaguaribe River flows through the entire state of Ceará disemboing into the Atlantic Ocean.
169 The study area sits between the latitudes of -6.5 and -7.5. The altitudes in the region vary from
170 approximately 300 to 870 m, with an average elevation of 550 m.a.s.l.

171 According to Köppen the climate of the region is defined as semi-arid dry and hot (“Bsh”)
172 (Araújo and Medeiros, 2013). It is characterized by a clear distinction between a rainy and a
173 dry season. The rain period lasting from January through May accounts for about 80% of the
174 total annual precipitation, which ranges from 500 to 1000 mm (Araújo and Medeiros, 2013),
175 amounting to 700 to 800 mm on average (Malveira et al., 2012). The dry season, however, is

176 characterized by water scarcity as the potential evaporation exceeds precipitation by up to four
177 times annually (Gatto, 1999). The prevailing climatic conditions with high interannual
178 precipitation variability cause regular droughts, which may even occur in several consecutive
179 years. Climate data and its pre-processing are presented in the Supplementary Material.

180 The vast majority of the region is covered by steppe-like savannah (Gatto, 1999). The
181 predominant natural flora is the so called arboreal *caatinga*, a vegetation type found only in the
182 Northeast of Brazil being composed of trees, shrubs and cacti, which are characterized as
183 tropical xerophytic deciduous broadleaved plants (Malveira et al., 2012; Gatto, 1999). The
184 *caatinga* presents a spatially rather continuous vegetation cover only with slight variations in
185 density. The trees have densely branched stems and firm foliage, which dries out and falls off
186 shortly after the rainy season (Güntner, 2002).

187 Geologically, 80% of the UJB is composed of crystalline bedrock (Eudoro, 2009), which
188 is characterized by shallow overlying soils with low hydraulic conductivity and porosity (Silva
189 et al., 2007). Therefore, the subsurface water storage (vadose zone and groundwater) in the
190 catchment is limited (Eudoro, 2009). Along the principal rivers and tributaries, alluvial
191 depositions may be found composed by young sandy-clayey sediments. These alluvial bodies
192 present rather high permeability (Feitosa, 1998; Feitosa and Oliveira, 1998; Colares and
193 Feitosa, 1998). Soil mapping and its physical parameters derivation are presented in the
194 Supplementary Material.

195 The spatial and temporal variability in rainfall, combined with the low groundwater storage
196 capacity and high evaporation, creates an adverse environment with regard to natural water
197 availability, which is characterized by intermittent rivers and low runoff coefficients (Araújo
198 and Medeiros, 2013; Malveira et al., 2012). Surface runoff generated in higher parts of the
199 hillslopes is likely to infiltrate into the soil when reaching lower unsaturated areas. If produced
200 at all, streamflow in upstream tributaries is of ephemeral nature, lasting only for short periods

201 (in the range of minutes). Only after several consecutive rainy days, the soil water content is
202 increased so that hydraulic connectivity is established on a catchment-scale and streamflow
203 occurs in the main rivers, continuing over longer periods (in the range of weeks) (Araújo and
204 Medeiros, 2013; de Figueiredo et al., 2016). In river reaches embedded in an alluvium the flow
205 regime is additionally influenced by channel transmission losses as a consequence of
206 infiltration through the river bed and banks (Costa et al., 2012, 2013).

207

208 **[Figure 1 is around here]**

209

210 ***2.2 Study area: reservoir system***

211 Reservoirs were distinguished between the large so-called *strategic reservoirs*, constructed
212 and managed by the state government, and the privately built, unmanaged reservoirs of
213 different sizes and shapes (Figure 1). The latter ones will be generally referred to as *small*
214 *reservoirs*.

215

216 ***2.2.1 Strategic reservoirs***

217 Four strategic reservoirs, namely Poço da Pedra, Benguê, Mamoeiro and Do Coronel, are
218 located within the catchment (Figure 1) with a drainage area of 800, 1,062, 1,888 and 25 km²,
219 respectively (Table 1). The daily storage volume and the flooded area for each strategic
220 reservoir are derived from the monitoring of water levels. The dam constructions usually
221 dispose of two different release facilities (Table 1): a drain unit with an adjustable clasp device
222 and an uncontrolled spillway.

223 Time series of the controllable releases are available for three of the strategic reservoirs
224 (Poço da Pedra, Do Coronel and Benguê). For Poço da Pedra and Do Coronel, no released
225 discharges occurred for the entire period. The records for Benguê showed some days, during

226 which water was released. No regularity was discernible and the discharges were rather small
227 (usually lower than 100 l/s). As the released discharges are negligibly small compared to the
228 observed streamflow and to the losses caused by lake evaporation (Güntner et al., 2004), they
229 were disregarded for the calculation of reservoir water balance. Differently from the
230 controllable water releases, the spillway overflow is quite relevant to estimate the reservoir
231 water balance, since large flood events were recurrent during the study period.

232

233 **[Table 1 is around here]**

234

235 ***2.2.2 Small reservoirs***

236 For previous studies on the reservoir network in the UJB (Mamede et al., 2012; Peter et al.,
237 2014), a total number of 230 reservoirs was registered in the Conceição River Catchment
238 analyzing aerial images taken immediately after the rainy season of the three comparatively
239 wet years 2004, 2008 and 2009. This analysis allowed the estimation of the maximum water
240 surface and the corresponding perimeter of the lakes. In-situ measurements of volume, area
241 and height of the small reservoirs are not available.

242 As the flooded areas represent a moisture state shortly after the rainy season of extremely
243 wet years, it was assumed that they correspond to the maximum capacity, beyond which water
244 is spilled from a reservoir (Mamede et al., 2012; Peter et al., 2014). Hence, an estimation of
245 the storage volumes based on these surface areas was conducted to gain the input data required
246 by the hydrological model. Simplified approaches to estimate the storage capacity and,
247 additionally, the spillway width are shown as follows.

248 **Storage capacity estimation:**

249 Molle (1994) conducted an extensive field study on the geometry of reservoirs in four states
250 of the semi-arid Northeast of Brazil, including the state of Ceará. Based on this work, he

251 developed the following equations describing the relation between surface area, height and
252 volume of a reservoir as a function of two parameters:

253

$$254 \quad V = k \cdot h^\alpha \quad (\text{Eq. 1})$$

$$255 \quad A = k \cdot \alpha \cdot h^{(\alpha-1)} \quad (\text{Eq. 2})$$

256 - V : estimated reservoir volume [m³]

257 - k : aperture coefficient

258 - h : reservoir height / water stage [m]

259 - α : shape coefficient

260 - A : surface area [m²]

261 When combining the two equations, one obtains an expression for the reservoir volume as
262 a function of the surface area (Pereira, 2017):

$$263 \quad V = k \cdot \left(\frac{A}{\alpha \cdot k}\right)^{\left(\frac{\alpha}{\alpha-1}\right)} \quad (\text{Eq. 3})$$

264 The two coefficients are site specific and vary depending on the prevailing topography.
265 Molle (1994) determined these coefficients for a sample of 420 reservoirs with capacities
266 ranging from 0.03 to 0.66 hm³. The mean value of the sample for α and the median for k
267 amounted to 2.7 and 1500, respectively. Using these parameters, the equation has been
268 commonly applied in many studies (e.g. Malveira et al. 2012, Peter et al. 2014).

269 In order to find mean values for the two coefficients of Molle's equation that are more
270 representative for the reservoir dimensions found in the Conceição River Catchment (reservoirs
271 with flooded area till 0.07 hm²), which are rather smaller than those from the sample of Molle
272 (1994), a sub-sample of 21 reservoirs from a database published by the Brazilian National
273 Department of Constructions against Droughts (Departamento Nacional de Obras Contra as
274 Secas - DNOCS) (Pinheiro, 2004) was taken at hand. The average value for α , 2.7, and the
275 median for k , 5046, of this sample were determined and adopted for this work. The estimated

276 storage capacity of the small reservoirs detected by aerial images in the catchment, based on
277 Molle's equation, ranges from 2,362 to 1,939,301 m³. The mean and median storage capacity
278 of the small reservoirs are 80,335 and 23,700 m³, respectively.

279

280 **Spillway width estimation:**

281 Not only the strategic reservoirs dispose of spillway structures, but the private non-operated
282 dams as well, even though their flood water release is generated in different manners. The small
283 reservoirs usually have a lowered sill made of compacted soil. Some reservoirs simply spill via
284 a natural or excavated so-called preferential flow channel. No information is available on the
285 width and the height of spillways of small reservoirs. So, in order to realize a broad-scale
286 assessment of the small-reservoir spillway widths, measurements based on satellite images
287 were conducted in Google Earth in cases where a spillway was clearly discernible from the
288 flight perspective.

289 After the satellite image analysis, only 21 measurements were considered, because in the
290 majority of cases no clear distinction between dam and spillway was discernible, mainly due
291 to the fact that both structures are made of earth and hence no difference in depth was
292 recognizable. Additionally, some of the larger reservoirs dispose of tubes integrated into the
293 dam, which could also not be assessed in the imagery. Aiming the estimation of all spillway
294 widths, it was assumed that the flood magnitude is related to the upstream drainage area. So,
295 all 21 values of Google-Earth-based spillway width were plotted against the upstream drainage
296 area of each dam obtained from a geographic information system (GIS). After removing three
297 outliers, a linear function was fitted to the plot with a coefficient of determination of 0.88.
298 Based on the thus obtained relationship, the width of the spillway of other small reservoirs
299 could be approximately determined entering the respective drainage area. With this width, the
300 released discharge based on the water stage over the spillway crest may be calculated.

301 However, it must be stated that the relation between width and drainage area represent only a
302 very rough estimation. It presents a source of uncertainty originating from the low resolution
303 of the satellite images in some regions, the potential misinterpretation of them and measuring
304 imprecision.

305

306 ***2.3 Model of the system of reservoirs and ponds***

307 ***2.3.1 Catchment delineation including reservoirs***

308 For simulating hydrological processes and reservoirs in the catchment, the model SWAT
309 was used. The delineation of the watershed and the definition of its river network (Figure 1)
310 were done in ArcSWAT based on a digital elevation model (DEM) with 90 m resolution.
311 Outlets of strategic reservoirs were incorporated as nodes. In this section, the model
312 development and parameterization of ponds and reservoirs is presented. Strategic reservoirs
313 and main private reservoirs along the river network were implemented into the SWAT model
314 as “Reservoir” during the watershed delineation, while the other small ones were added as
315 “Pond” as they are situated on tributaries off the main river network (Figure 1).

316 The classification of small reservoirs as “Reservoirs” or as “Ponds” was done depending
317 on their impact on the generated water runoff. Water impoundments were implemented as
318 Reservoir, if they meet all of the following criteria:

- 319 i. The water impoundment is caused by a dam construction built across the main river
320 reach;
- 321 ii. The upstream drainage area of the reservoir is substantially larger than the average
322 design sub-basin area (~20 km²);
- 323 iii. The estimated storage capacity of the water impoundment is larger than 0.01 hm³.

324 In the special case that the water impoundment was complying with the first two criteria
325 but not with the third one, it was assigned to the second category (Pond) for means of

326 simplification, even though it was receiving water from upstream sub-basins. By implementing
327 these water impoundments as Pond, as if they were located off the main channel, their water
328 retaining effect was not completely neglected.

329 To implement the remaining reservoirs as Pond, the following criteria were checked:

- 330 i. The water impoundment is caused by a dam construction built across the river reach;
- 331 ii. The upstream drainage area of the reservoir is approximately equal or smaller than the
332 average design sub-basin area (~20 km²).

333 Fulfilling these criteria, a water impoundment was considered a pond according to the
334 SWAT definition. In case the upstream drainage area was larger than the designated minimum
335 sub-basin area (5 km²), the outlet was placed on the stream just downstream of the lake,
336 generating a sub-basin whose entire area drains into the pond allocated to it. Deliberately
337 placing certain ponds at the outlet of sub-basins simplifies further calculations for the
338 determination of their drainage fraction, which is a required input parameter for SWAT.

339 If no dam construction was detected, the water impoundment was disregarded in the model.
340 During a flood event, depressions in the landscape or flood plains may be inundated and filled
341 with water, being registered as a water impoundment through remote sensing. These inundation
342 lakes were neglected in the model as they show different topographic characteristics than the
343 lakes impounded by dams, which would lead to an overestimation of their storage volume when
344 applying the general method for volume estimation from flooded surface area (see section
345 2.2.2). This would then cause a distorted impact on the surface runoff.

346 The model catchment delineation ended up with a total of 191 dams and 197 sub-basins
347 (Figure 1). The average sub-basin size amounted to approximately 17 km². A total of 18 dams
348 were implemented as Reservoir (4 strategic and 14 main private) and 79 sub-basins contained
349 dams that were either individually assigned or aggregated as Pond.

350

351 **2.3.2 Aggregation of small reservoirs into ponds**

352 SWAT allows only one single pond to be allocated to each sub-basin. After the watershed
353 delineation, however, many sub-basins ended up containing multiple small reservoirs, that was
354 considered a reservoir system, in which it was distinguished between a cascade and a parallel
355 arrangement of reservoirs (Figure 2). In the cascade arrangement, two or more reservoirs are
356 located one behind the other on the same river reach. Water being released from the upstream
357 reservoir will flow into the downstream reservoir. So, the filling of a downstream reservoir
358 depends on the amount of water held up by reservoirs further upstream and thus on the storage
359 capacities and drainage areas of all upstream reservoirs. In the case that two or more reservoirs
360 are arranged parallel to each other, the filling and spilling processes are independent of each
361 other. In the parallel arrangement, each reservoir is located on a separate river branch of the
362 same order. Water being released from one reservoir does not flow into the other. Each
363 reservoir has a separate drainage area.

364

365 **[Figure 2 is around here]**

366

367 Based on the arrangement of small reservoirs and their drainage areas, certain calculation
368 rules were applied for the determination of the aggregated reservoir volume. Drainage areas of
369 downstream reservoirs were kept fixed, while the volumes were reduced if necessary. In that
370 way, it was guaranteed that only a fraction of the sub-basin contributes to runoff production
371 that actually does not drain into any reservoir. In the case that a pond is located directly at the
372 outlet, no outflow from the sub-basin will occur until the storage capacity of the aggregated
373 pond is exceeded.

374 With regard to the rarity and variability of runoff, it is plausible to assume that in some dry
375 years even some of the smaller reservoirs do not spill. So, it was aimed at estimating the mean

376 storage volume that has to be reached so that water is exiting a network of small reservoirs.
377 This volume will be referred to further on as *equivalent capacity*, the system's impact on the
378 hydrology will be termed *storage effect*.

379 Two extreme states may be distinguished with regard to the storage effect:

- 380 i. The state when the entire amount of generated runoff in the system is stored so that no
381 outflow occurs. This may be seen at the beginning of the rainy season. Only if a certain
382 threshold water volume is exceeded the system spills. This threshold storage may be
383 considered the *effective capacity*.
- 384 ii. The other state occurs after full saturation of the system (all reservoirs filled, high soil
385 moisture) after some consecutive rainy days. At this point, the system only damps the
386 outflow hydrograph, releasing the amount of water above the total storage capacity of
387 the system.

388 In other words, the effective capacity of the reservoir network determines whether it spills,
389 while the total storage capacity determines how much water is spilled. In order to simulate a
390 storage effect that will match the one in reality on average, it was set the equivalent storage
391 capacity of the lumped pond to a value in between effective capacity and total storage capacity.

392 If the relation of capacity to drainage area of an upstream reservoir is equal to or smaller
393 than that of the downstream reservoir (considering only the fraction of drainage area beneath
394 the upstream reservoir), the upper dam will spill first. Hence, the equivalent storage capacity
395 of the system amounts to the total capacity, the sum of both. This case corresponds to the
396 assumption of a positively constant relation between capacity and drainage area made for other
397 studies (e.g., Güntner et al., 2004; Zhang et al., 2012). In the case that this ratio is higher for
398 the upstream reservoir, the downstream reservoir will spill first. When assuming the drainage
399 area of the downstream reservoir, though, an addition of the single storage capacities would
400 lead to a strong overestimation of the effective capacity. Spilling from the sub-basin would be

401 simulated with delay or not at all. If only the downstream volume is considered the threshold
 402 storage for spilling of the system would be matched but the total capacity would be highly
 403 underestimated. In this case, the equivalent capacity is calculated as the sum between the full
 404 capacity of the reservoir with the larger specific drainage area and the other capacity reduced
 405 by the fraction of the two drainage areas (Eq. 4).

406
$$\text{if } \frac{V(R_u)}{DA_u} \leq \frac{V(R_d)}{DA_d} :$$

407
$$V_{eq} = V(R_u) + V(R_d)$$

408

409
$$\text{if } \frac{V(R_u)}{DA_u} > \frac{V(R_d)}{DA_d} :$$

410
$$\text{if } DA_u > DA_d: V_{eq} = V(R_u) + \frac{DA_d}{DA_u} \cdot V(R_d)$$

411
$$\text{if } DA_u < DA_d: V_{eq} = V(R_d) + \frac{DA_u}{DA_d} \cdot V(R_u)$$

412

413 - V_{eq} : equivalent storage capacity of aggregated pond

414 - $V(R_u)$: storage capacity of upstream reservoir

415 - $V(R_d)$: storage capacity of downstream reservoir

416 - DA_u : drainage area of upstream reservoir

417 - DA_d : drainage area of downstream reservoir

418

419 Accordingly, for a parallel arrangement of small reservoirs in the same sub-basin, if the
 420 relation of capacity to drainage area of two reservoirs is equal both will spill at the same time.
 421 Hence, the equivalent storage capacity of the system amounts to the total capacity, the sum of
 422 both. This case corresponds to the assumption of a positively constant relation between
 423 capacity and drainage area.

424 For the case that this relation is smaller for one of the reservoirs, this dam will spill before the
 425 other one. Assuming the sum of both drainage areas as an upstream basin for the lumped pond,
 426 the effective storage capacity would be overestimated. Considering only the drainage area and
 427 capacity of the reservoir with the smaller ratio the threshold storage for spilling would be
 428 matched, but the total capacity would be underestimated. In this case, the equivalent capacity
 429 is calculated in the same way as for the sequential configuration, as the sum of the full capacity
 430 of the reservoir with the larger specific drainage area and the other capacity reduced by the
 431 fraction of the two drainage areas (Eq. 5).

432
$$\text{if } \frac{V(R_1)}{DA_1} \approx \frac{V(R_2)}{DA_2} :$$

433
$$V_{eq} = V(R_1) + V(R_2)$$

434

435
$$\text{if } \frac{V(R_1)}{DA_1} \neq \frac{V(R_2)}{DA_2} :$$

436
$$\text{if } DA_1 > DA_2: V_{eq} = V(R_1) + \frac{DA_2}{DA_1} \cdot V(R_2)$$

437
$$\text{if } DA_1 < DA_2: V_{eq} = V(R_2) + \frac{DA_1}{DA_2} \cdot V(R_1)$$

438

439 - V_{eq} : equivalent storage capacity of aggregated pond

440 - $V(R_1)$: storage capacity of first reservoir

441 - $V(R_2)$: storage capacity of second reservoir

442 - DA_1 : drainage area of first reservoir

443 - DA_2 : drainage area of second reservoir

444 By these calculation rules, it was considered that if the combined drainage area is assumed,
 445 the storage effect of the reservoir with the larger drainage area is weighted higher for the
 446 estimation of the joint storage capacity. In case that multiple small reservoirs are arranged in

447 the same configuration or that the two arrangements are combined in one sub-basin, it was
448 started with the most upstream reservoirs. Their volumes were aggregated according to the
449 respective rule, then this intermediate equivalent volume was again lumped with the small
450 reservoir further downstream and so on.

451

452 *2.3.3 Parameterization of strategic reservoirs*

453 In SWAT, a reservoir is basically described by the principal volume (V_{pr}), the emergency
454 volume (V_{em}) and the respective flooded surface areas (SA_{pr} and SA_{em}). With these
455 parameters the surface-area-volume curve is calculated and the water release is determined.
456 The gradual flood water release from the strategic reservoirs may best be modeled in SWAT
457 with the target release for controlled reservoir function (IRESCO=2). The outflow routine
458 allows a gradual spilling of the water volume above a certain target volume (V_{targ}) and under
459 the emergency volume (V_{em}). The maximum storage capacity of each reservoir, corresponding
460 to a water level equal to the height of the weir crest, was set as V_{pr} . Considering that the
461 spillways of all reservoirs in the catchment are uncontrollable free weirs, V_{targ} was fixed as
462 V_{pr} for all months. In order to guarantee a gradual water release over the spillway, V_{em} must
463 be set substantially higher than V_{pr} so that it is possibly never exceeded. V_{em} and SA_{em} are
464 available for strategic reservoirs by the state water agency.

465 The parameter NDTARG, representing the number of days required for releasing all excess
466 water above V_{targ} , determines the amount of water flowing out from the reservoir on each day.
467 It depends on the type and the width of the spillways. In order to find a value for this parameter,
468 daily spillway discharges for different excess volumes were calculated for each strategic
469 reservoir. The discharge over the spillway in SWAT was calculated according to the commonly
470 known weir overflow Poleni equation (Aigner, 2008), which depends on the width and the
471 form of the spillway (Table 1). The weir-type-specific overflow coefficients were set according

472 to the weir types: 2.1 for Benguê and Mamoeiro, 1.75 for Poço da Pedra and 1.6 for Do Coronel.
473 Water levels were considered only up to a height slightly above the maximum observed
474 elevation in the provided time series of the reservoirs: 1 m above the spillway crest for Benguê
475 and Mamoeiro, 0.75 and 0.5 m for Do Coronel and Poço da Pedra, respectively. Excess
476 volumes were also calculated for water stages at 0.01, 0.05, 0.10, 0.25 and 0.50 m above the
477 spillway for all strategic reservoirs.

478 Therefore, the Poleni equation was solved for half-hourly time steps, readjusting the water
479 stage after each step based on the specific volume-elevation-curve. The amounts of water
480 released after each time step were added up, obtaining the total water volume released in one
481 day. The values for the excess volume, i.e., the volume above reservoir capacity, were then
482 plotted against the values for the calculated released water volume. Linear functions were fitted
483 to the plots (Figure 3), with NDTARG equal to the inverse of the slopes of the straights. The
484 straight lines presented high coefficients of determination ($R^2 > 0.9$), which led to the
485 conclusion that the spilling behaviour of such reservoirs could be suitably represented by the
486 function implemented in SWAT.

487 The obtained values for NDTARG reveal that all the excess water is released within slightly
488 more than one day for the reservoirs Benguê and Do Coronel. Mamoeiro spills all the excess
489 water in less than one day. For the excess water to be released from Poço da Pedra, however,
490 it takes more than two days. These statements are only valid for the assumption that no water
491 is entering the reservoir during this time. In reality, the spilling process is much more dynamic.
492 A simulation on hourly time steps would be much more precise, but would lead to high
493 computation time. As the simulation step in SWAT was set to one day due to data availability
494 limitations, the approach presented here was considered the most appropriate way to estimate
495 the daily released water volume.

496

497 **[Figure 3 is around here]**

498

499 The parameters IYRES and MORES (year and month, in which the reservoir was built,
500 respectively) were set according to the available information. The parameter EVRSV, the lake
501 evaporation coefficient, was set to 1, which represents the maximum value, to guarantee high
502 evaporation losses. The parameter RES_K represents the hydraulic conductivity of the
503 reservoir bottom. It determines the losses through infiltration. Due to the professional planning
504 and construction of the governmental reservoirs, it was assumed that these dams were
505 sufficiently sealed and RES_K was set to 0.

506 The initial reservoir volume (parameter RES_VOL) for Benguê was obtained from
507 recorded values shortly after the reservoir became operational in 2000. The initial storage
508 volume represented about 4 % of its capacity. For Mamoeiro, which became operational in
509 2012, the initial volume was also set to 4 % of its capacity. However, no further time series
510 were available for Mamoeiro. For Do Coronel, the observed storage volume on the first day of
511 simulation in 1979 was obtained from the available records.

512 The time series for Poço da Pedra showed a gap for the years around 1979. The storage
513 volume at that time was estimated based on all other values registered at the beginning of
514 January in the other years and based on the rainfall measured in 1978. The mean annual rainfall
515 was calculated from five rain gauges inside the study catchment both for the year 1978 and for
516 the entire simulation period. The annual rainfall in 1978 showed to be around 71 % of the mean
517 annual rainfall of the entire simulation period. The average of registered reservoir volumes at
518 the beginning of January amounted to 46 % of the total capacity. So, the initial storage for Poço
519 da Pedra was estimated with these percentages: $RES_VOL = 0.71 \times 0.46 \times \text{capacity}$. Table 2
520 summarizes the parameterization of reservoirs, with a description of all parameters.

521 The representation of the withdrawal of water from the reservoirs was considered in the
522 model in a simplified approach: urban water supply and irrigation were represented by a
523 constant monthly water withdrawal based on state water agency data for each strategic
524 reservoir.

525

526 **[Table 2 is around here]**

527

528 *2.3.4 Parameterization of main private reservoirs*

529 Except for the flooded areas measured through remote sensing at the end of the flood season
530 of extremely wet years, no data were available on the 14 main private reservoirs, which were
531 implemented as Reservoir into the SWAT model. As they typically dispose of some type of
532 spillway, it was assumed that the water storage effect of these dams was similar to that of the
533 strategic reservoirs. So, their implementation followed the same principle.

534 The measured flooded area was set as S_{Apr} and the respective volume, which was therefore
535 estimated using the Molle-based approach, was assumed as capacity and set as V_{pr} . Moreover,
536 the volume corresponding to a water level of 1.5 m above the crest of the spillway was
537 calculated and assumed as V_{em} . The height of 1.5 m was assumed as a reasonable value for
538 the average height between spillway and dam crest.

539 Assuming the same procedure of overflow analysis that was followed for the strategic
540 reservoirs and general simplifications of spillway geometric properties, it was found that the
541 excess water is spilled within less than one day for almost all small reservoirs, i.e., less than
542 the model calculation time step. The average NDTARG parameter was set as 1 for the main
543 private reservoirs.

544 The application *Google Timelapse* was used to determine, in which year each reservoir was
545 built, setting IYRES accordingly. This *Google* function provides satellite images of many

546 regions from the years 1984 until 2017. If it was seen that a dam had been present since 1984,
547 it was assumed that it had been existing since 1979. In these cases, MORES was set to January.
548 In the other cases, MORES was set to November, the ending of the dry season, assuming that
549 the dams are constructed during the dry season.

550 According to Molle (1989), seepage does not occur in the flooded area of the reservoir due
551 to the underlying crystalline bedrock but rather underneath the dam along the original river
552 bed. In the study, the insufficient sealing and compaction of the dam structures were concluded
553 to be the principal reason for infiltration losses. So, the seepage process implemented in SWAT,
554 assuming a loss through the flooded area (Neitsch et al., 2009), does not adequately represent
555 the infiltration process happening in the field. In order not to neglect seepage losses from small
556 reservoirs, however, the SWAT parameter RES_K (hydraulic conductivity of reservoir bottom)
557 was set according to the average seepage rate found in Molle (1989), which amounted to 2.64
558 mm per day (0.1 mm per hour). For evaporation losses, the same value of 1 for EVRSV was
559 defined, as described for strategic reservoirs.

560 Reservoirs that were built during the simulation period were assigned 0 as initial storage
561 volume. For the other reservoirs, the initial storage was set according to the size class (same as
562 used in the studies presented here). Micro-dams (capacity $< 0.1 \text{ hm}^3$) were assumed to be empty
563 before the flood season (in January), small-sized dams ($0.1 \text{ hm}^3 < \text{capacity} < 1 \text{ hm}^3$) were
564 assumed to be at 10 % of their capacity and the medium-sized ones ($1 \text{ hm}^3 < \text{capacity} < 10$
565 hm^3) were assumed to be at 20 % of their capacity. The remaining parameters were left as
566 SWAT default. A summary of the main private reservoir parameters can be found in Table 2.

567

568 *2.3.5 Parameterization of ponds*

569 The obtained equivalent capacity of a system of small reservoirs was set as the V_{pr} of the
570 aggregated pond of each sub-basin. The corresponding equivalent surface area was determined

571 according to the same calculation rules, setting it as the SApr of the lumped pond of each sub-
572 basin. With the single reservoir volumes corresponding to a water level of 1.5 m above the
573 spillway Vem and SAem of the aggregated ponds were calculated using the same method.

574 In SWAT, it is not possible to set the date when a pond came into being. So, it had to be
575 assumed that all ponds had been existing since the beginning of the simulation period, which
576 adds another source of uncertainty considering the transient nature of the micro-dams and
577 looking at the development of dam construction in the region analysed in Malveira et al. (2012).

578 Based on the considerations made for reservoir bottom percolation, the respective
579 parameter for infiltration through the pond bottom (K_POND) was set as 0.1 mm/h, too. From
580 the investigation about the spilling behaviour, it was found that only above the threshold value
581 of 0.01 for the ratio of capacity to drainage area of the single small reservoirs, it takes more
582 than one day for the excess volume to be spilled (NDTARG > 1.0). From the highest value for
583 NDTARG and the lowest one with the corresponding ratios, a linear relation was set up. Based
584 on this equation the NDTARG parameter was determined for all the small ponds that showed
585 a ratio higher than 0.01. In case the pond was located at the outlet of a sub-basin, the
586 interpolated value for NDTARG was assumed for the aggregated pond in the respective sub-
587 basin. For the remaining sub-basins with ponds, the parameter was set to 1.

588 Initial storages of the aggregated ponds were also set based on the single small reservoirs
589 located in the sub-basin, following the reservoir-size class as aforementioned. If at least one
590 small reservoir of a higher reservoir size-class (small- or medium-sized dam) is located in a
591 sub-basin, the initial storage was set as a fraction of the capacity of this reservoir, accordingly.

592 Table 3 summarizes the parameterization of ponds.

593

594 [Table 3 is around here]

595

596 *2.4 Parameterization of dryland hydrology*

597 *2.4.1 Model calibration approach*

598 The aim of the calibrated model is to describe the rainfall-runoff relationship of the
599 catchment with the reservoir system as a base for further investigations and scenario
600 simulations. Studying the sensitivity and uncertainty of hydrological parameters is not the
601 subject of this study.

602 Based on the available data, literature and the experience of the modelers, the following
603 methods were chosen for the calculation of infiltration, evapotranspiration and channel routing,
604 respectively: Curve Number Method, Plant Evaporation Method and Muskingum Method.

605 The parameters of the model were calibrated with an iterative trial and error procedure with
606 the objective of maximizing statistical model performance and minimizing bias in stream flow,
607 by keeping parameter values in a physically meaningful range. Initial values for the model
608 parameters were derived from field data as much as possible. Then, where field data from the
609 case study area were not sufficient, values from literature about dryland catchments were
610 chosen to represent the characteristics of the study catchment. Finally, remaining sensitive
611 parameters were calibrated.

612 The model was calibrated separately for the sub-catchments of the three large strategic
613 reservoirs Benguê, Poço da Pedra and Do Coronel. The simulated reservoir volume was
614 compared to the time series for the strategic reservoirs. As the Mamoeiro reservoir became
615 operational only in 2012, after the last year of the Malhada station available time series (1979
616 – 2010), it was disregarded for the presented analysis. The remaining sub-basins were sub-
617 divided into three categories: upstream sub-basins with mountainous river reaches, transition
618 sub-basins with medium-order river reaches and down-stream sub-basins. The sub-division
619 was done by personal judgment with regard to the topography, slope classes and the order of
620 the river reaches.

621 It is common in hydrological modeling to use warm-up periods, especially when the initial
622 simulation conditions are not known. A warm-up is a sufficient period to run the model to
623 initialize important variables or allow processes to reach a dynamic equilibrium. The
624 complexity of watershed-scale processes impact the length of warm-up periods for
625 hydrological models. However, two to four years are recommended by model developers due
626 to having a complete hydrological cycling in the modeling. These periods are used by SWAT
627 modelers in the arid and semiarid region for hydrological studies (Daggupati et al., 2015;
628 Jajarmizadeh et al., 2017; Zettam et al., 2017; Kim et al., 2018; Mendoza et al., 2021; Mengistu
629 et al., 2021).

630 The calibration and validation of the model was performed using the technique of two-fold
631 cross-validation. Considering the first two years as a warm up of the model simulation (1979
632 and 1980), the first half of the series (1981 - 1995) was used for calibration, while the second
633 half (1996 - 2010) was used for validation, obtaining the statistical criteria for both series at
634 the Malhada station. Subsequently, the second half of the series was used for calibration, while
635 the first half was used for validation.

636 The reservoir volume simulation was evaluated for the whole series, but with a special
637 highlight in the periods when each reservoir spilled out. These periods have a greater
638 importance due to the spillway overflow directly influencing the streamflow at the outlet of the
639 catchment. The simulated and observed time series of the reservoir's volume were overlain and
640 their fitting was visually evaluated.

641 The years considered in the series for two-fold cross-validation have periods of flood and
642 drought, such as 1985 and 2004 (rainy years) and 1993 and 2005 (drought years). These rainy
643 years were extremely wet years, when all strategic reservoirs spilled out. Beyond these extreme
644 years, the preceding and following years were moderately wet to dry. In this way, the model
645 could be evaluated for different extreme seasons and rainfall events.

646 For the calibration procedure, the daily simulated stream flow were tried to match the daily
647 observed stream flow at Malhada gauging station, evaluating the plausibility of the magnitude
648 and the duration of the uncontrolled released discharges by reservoirs with regard to the stage-
649 discharge curves (i.e., excess-volume-to-released-volume-curves) developed in this work. To
650 assess the fitting of daily streamflow hydrographs (observed vs. simulated), a combination of
651 three quantitative statistical criteria commonly applied in hydrological modeling was used: the
652 percent bias (PBIAS), the Nash-Sutcliffe-Efficiency (NSE) and the Kling-Gupta-Efficiency
653 (KGE).

654

655 ***2.4.2 Rainfall-runoff process, flood routing and channel transmission losses***

656 The dominant vegetation *Caatinga* resembles the vegetation type rangeland. The
657 Manning's roughness coefficient for overland flow for rangeland with 20% vegetation cover
658 was provided in Neitsch et al. (2009). The maximum canopy storage (CANMX) was set to 1.5
659 mm as the average value for canopy storage in an arid environment stated in Attarod et al.
660 (2015). The parameters SOL_AWC (available water capacity) and SOL_K (saturated hydraulic
661 conductivity) were derived by applying pedo-transfer functions (PTF) based on Brazilian
662 literature for each soil layer (Supplementary Material). Three soil types (Latosol Vermelho
663 Amarelo, Bruno não-Calcio and Litolicos Eu Textura Arenosa) had characteristics of vertic
664 soils. For them, the bypass flow function of SWAT was activated.

665 For a reach of the Middle Jaguaribe River, Costa et al. (2013) found that at the end of
666 regular/moist rainy seasons, the river becomes a losing/gaining system, with its streamflow
667 being sustained from base flow occurring in the underlying alluvium. The test reach
668 represented a high order river in lower areas. As the principal rivers and tributaries in the study
669 catchment are embedded in layers of alluvium as well, similar effects of streamflow being
670 sustained by backflow from these alluvium bodies may also be expected. Therefore, river

671 reaches were classified into three orders in the model: high order reach, medium order reach,
672 and upstream tributary. SWAT allows to calculate water movement from the shallow aquifer
673 to the root zone, which is controlled by the groundwater “revap” coefficient (GW_REVAP).
674 For the respective sub-basins, the GW_REVAP was set accordingly to different values,
675 decreasing in magnitude with increasing reach order.

676 According to the findings in Costa et al. (2013), transmission losses increase with
677 increasing discharges due to a higher hydraulic head. In order to include a more appropriate
678 approach for transmission losses on a catchment scale, the parameters CH_K2 (effective
679 hydraulic conductivity of the channel alluvium in main river reaches) and CH_N2 (Manning’s
680 roughness coefficient for main channels) were set to different values depending on the
681 topographic position of the sub-basins and the slope classes in the vicinity of the main river
682 reaches.

683 The calibration of other parameters, such as ESCO (soil evaporation compensation
684 coefficient), ALPHA_BNK (bank flow recession coefficient), ALPHA_BF (base flow
685 recession coefficient), GW_DELAY (delay time for aquifer recharge), GWQMN (threshold
686 water level in shallow aquifer for base flow), REVAPMN (threshold water level in shallow
687 aquifer for evaporation) and TRNSRCH (fraction of the transmission losses partitioned to the
688 deep aquifer) can be seen in a summary in the Tables 4, 5 and 6. Table 4 presents parameters
689 set for the entire catchment. Table 5 presents parameters set for specific sub-basins of the
690 catchment, with distinction between sub-catchments of two strategic reservoirs and
691 topographic position of sub-basins. Table 6 presents parameters set for specific zones in the
692 catchment, with distinction between soil types.

693

694 **[Table 4 is around here]**

695

696 [Table 5 is around here]

697

698 [Table 6 is around here]

699

700 *2.5 Reservoir scenarios*

701 One of the goals of this investigation is to assess the impact of the small reservoirs (ponds
702 and main private reservoirs) on the model streamflow and volume series. As the estimate of
703 those structures was made mainly with the help of aerial images, there is considerable
704 uncertainty in this process.

705 Thus, in order to investigate different scenarios for the dimensions of the small reservoirs
706 (RES_ESA, RES_EVOL, RES_PSA, RES_PVOL and RES_VOL) and ponds (PND_PSA,
707 PND_PVOL, PND_ESA, PND_EVOL and PND_VOL), their volumes were multiplied by
708 factor zero and the factor ten. These parameters represent areas and volumes that were
709 estimated by the analysis of aerial images in the model (see section 2.2.2). “0 time” means the
710 total absence of small reservoirs and was chosen to show how the model behaves without these
711 small reservoirs. “10 times” means a ten times increase in the aforementioned parameters that
712 represent the volumes of these small reservoirs. With these modifications, the model was run
713 from 1979 to 2010 to assess their impact on the simulation of the streamflow at the Malhada
714 station and of the volumes and the spillway overflows for the strategic reservoirs. We especially
715 evaluated the peak values of the streamflow hydrograph at the Malhada station and the number
716 of days of spillway overflow in the strategic reservoirs.

717 In addition, another scenario approach was performed to assess the impact of the reservoirs
718 on the simulated streamflow at the outlet. The general influence of reservoirs was performed
719 considering 4 scenarios: (i) considering all strategic reservoirs and small reservoirs (reference);
720 (ii) removing all small reservoirs in the hydrological system, but keeping only the strategic

721 reservoirs; (iii) removing all strategic reservoirs but keeping only the small reservoirs; (iv)
722 removing all reservoirs. The model was run for the whole series with these hypothetical
723 scenarios [(ii), (iii) and (iv)] and the streamflow at Malhada station was compared with the
724 reference scenario (i).

725 Figure 4 illustrates the main flowchart of this study, with a summary of all methods applied.

726

727 [Figure 4 is around here]

728

729 **3 Results and Discussion**

730 ***3.1 Simulation of streamflow***

731 The most relevant parameters in SWAT simulations in this study were identified as
732 SOL_CRK, TRNSRCH, CH_K2, LAT_TIME, REVAPMN, GW_REVAP and CH_N1. It is
733 worth mentioning that CN2 showed only low sensitivity even though it was often reported as
734 very sensitive in other catchments. We explain that with the climatic and soil characteristics of
735 the area, where soil moisture and infiltration processes more often underlie extreme dry or wet
736 conditions than elsewhere. In this study, the first two years (1979 and 1980) were considered
737 as warm-up period for adjustment of internal processes (e.g., soil moisture redistribution) that
738 moves from an estimated initial condition to a realistic state. The model performance during
739 the two-fold cross-validation periods was assessed with the three previously presented
740 statistical performance criteria. Table 7 presents the obtained values for each for the
741 calibration-validation periods. These values indicate a good model performance. The analysis
742 of the values for both NSE and KGE attested a good overall fit of the simulated and observed
743 hydrographs at Malhada station. The model simulated streamflow peaks with fairly high
744 accuracy with regard to their dates of occurrence and their magnitudes. When calibrating the
745 model with the first half of the series (1981-1995) the model overestimated streamflow values

746 (highly negative PBIAS) for the second half (1996-2010); when calibrating the model with the
747 second half of the series (1996-2010) the model underestimated the streamflow values (highly
748 positive PBIAS) for the first half (1981-1995).

749

750 **[Table 7 is around here]**

751

752 Figure 5 depicts the observed and the simulated hydrographs for the calibration-validation
753 periods, while Figure 6 depicts the log flow duration curve for these periods. For better display,
754 Figure 7 shows close-ups of hydrographs with a logarithmic scale streamflow for the single
755 years (1985 and 2004) during which relevant discharges were observed. These years were
756 chosen because they represent the wettest years, allowing a full analysis of the hydrograph
757 rising limb, the peak flow and the recession flow. For dry years, with low precipitations, and
758 consequently low flows, the analysis of these hydrograph characteristics would be limited.
759 Figures 5 (a, b), 6 (a, b) and 7 (a, b) present results for 1981-1995 calibration and 1996-2010
760 validation and (c) and (d) in both figures present results for 1996-2010 calibration and 1981-
761 1995 validation. For Figure 7, only the first half of the year, the wet season period, is presented
762 as for the rest of the year neither observed nor simulated discharges occur (the dry season). It
763 is remarked that the scale of the vertical axis is adapted for each year.

764

765 **[Figure 5 is around here]**

766

767 **[Figure 6 is around here]**

768

769 **[Figure 7 is around here]**

770

771 The results show that the model was able to simulate dry years in which no or only minor
772 discharges are registered (1983, 1993, 2001 and 2005) at the Malhada gauging station. For
773 these years no water reached the outlet of the catchment, so the hydrograph was not presented
774 here. This indicates that both the storage capacity of the single reservoirs and the losses due to
775 evapotranspiration and riverbed infiltration were estimated sufficiently high. For years with
776 near-average water yield, the model accuracy was good for some years (1984, 1987-1988,
777 1990, 1992, 1994, 1996, 1999 and 2003), but was rather poor in others (1986, 1989, 1995,
778 1997, 2000, 2002 and 2006-2008). For these years with worse accuracy, until 2002 the peak
779 streamflow was underestimated, which means that the observed streamflow has higher peaks
780 and more water reaching the outlet. From 2006 to 2008 the model overestimated the peak
781 streamflow. These results can be seen in Figure 5. For 2009, the modeled peak was clearly
782 overestimated.

783 The graphs clarify that for wet years during which the large reservoirs spilled out (1985
784 and 2004) the days of extreme flood events (high peaks) were matched with high accuracy by
785 the model. The magnitude of the simulated peaks was within a similar range than those of the
786 observed ones. However, the flow recession was not well represented by the model. It was
787 found that it is characteristic for the study area that the streamflow lasted for many days after
788 strong consecutive rain events. The abrupt recession of the simulated hydrograph at the end of
789 wet periods, with streamflow going down to zero just after a few days the peak occurred in all
790 simulation results, while in the observed hydrograph the streamflow lasts for a few days. After
791 extremely rainy periods, water accumulates in the regions close to the river channel, forming
792 flood plains. The river recharge process after this period is notably complex, with unsaturated
793 seepage and vertical unsaturated subsurface water redistribution beneath the stream, lateral
794 stream-aquifer interaction and groundwater flow, parallel to the river course, in unconfined
795 aquifers. These processes and the channel transmission losses for arid and semi-arid watersheds

796 are very simplified in the SWAT model and have a great influence on these basins (Costa et
797 al., 2012).

798 Some of the years with moderate rain showed worse accuracy in peak streamflow,
799 hydrographs limbs and recession flow, either with underestimation or with overestimation in
800 the simulated values, depending on the year of analysis. Those years with near-average
801 streamflow require attention in the hydrological simulations, mainly due to the possible
802 unsaturated characteristics of the soil. Transmission losses are more complex in these years
803 and the SWAT model equation is relatively simple, depending on hydraulic conductivity, flow
804 translation time, wet perimeter and channel length. Uncertainties in the input data were one of
805 the difficulties during modeling in this dryland catchment, mainly in the values of hydraulic
806 conductivity. The values of hydraulic conductivity and transmission losses estimated also
807 affected the recession flow, whose simulated values also showed streamflow results with
808 sharper drops than the observed values in the hydrographs after the rainy season. In all cases,
809 there is uncertainty in rainfall data (lack of continuous rain gauge monitoring in some days and
810 human errors in measurements) although the 44 stations available in the catchment can reduce
811 errors. No significant errors were found. Despite that, errors of rainfall data during storm events
812 can significantly impact modeling. Even interpolation cannot compensate for gaps in the
813 recording of the local variability of rain.

814

815 ***3.2 Simulation of reservoir volume***

816 The simulated storage volumes during the cross-validation of the three strategic reservoirs
817 Poço da Pedra, Benguê and Do Coronel are presented for comparing their values and temporal
818 dynamics with the observed values based on data availability and operation periods (Figure 8).
819 From the diagrams, it can be seen that the peaks during flood year 2004 were matched well for
820 the three reservoirs. The model simulated the filling of the reservoir very well until the storage

821 capacity was exceeded. For the other years, the model simulated that the capacity was exceeded
822 for 1986, 1988-1990, 1997 and 2009-2010 for Poço da Pedra, 2006-2009 for Benguê and 2009
823 for Do Coronel. Analyzing Figure 8, the storage volume in Poço da Pedra and Benguê
824 reservoirs was higher overestimated in some years, besides the periods that the simulated
825 storage of the reservoir reached the maximum volume (1988-1990, 1997 and 2009-2010 for
826 Poço da Pedra and 2006-2007 for Benguê), when the observed data showed a value quite distant
827 from that. The evolution of the hydrograph, however, was well represented by the model. For
828 Do Coronel, the curve of simulated storage volume showed slightly overestimated values
829 compared to the observed ones for the years after and before the flood years. The overall
830 dynamics is better simulated than for the other two reservoirs.

831 Despite these differences in storage volumes of Poço da Pedra and Benguê, we did not find
832 any systematic error. The years of 1997, 2008 and 2009, for example, showed considerable
833 streamflow at Malhada gauging station, while the years of 1998, 2001 and 2010 showed low
834 streamflow. There were no direct discharge measurements upstream from the studied
835 reservoirs. Storage volumes were used to validate the reservoir modeling approach. On the
836 other hand, from 2008 to 2010 the model overestimated the storage volumes in Poço da Pedra,
837 as well as the streamflow at Malhada gauging station in these years, especially in 2009. Some
838 characteristics of dryland environments cause uncertainties for modeling of rainfall-runoff
839 processes, for example the nonlinear behavior of runoff generation and the irregular spatial
840 patterns of soil properties (Rödiger et al., 2014; Mamede et al., 2018).

841 The fall of the storage volume during the dry period, too, was modeled very realistically.
842 For the years before and after a flood year, the curves fitted very well for reservoirs. The slope
843 of the curve after a rainy season was a little more pronounced in the model. This period is
844 characterized by intense evaporation and a decrease in the volume of the reservoirs for semiarid

845 sub-basins and the parameter that calculates the evaporation (EVRSV) in the reservoirs in the
846 model was established at the highest possible value (see Table 2).

847 The catchment of Benguê reservoir was modeled by Mamede et al. (2018) using the
848 WASA-SED model (Güntner et al., 2004; Bronstert et al., 2014) for the period 2000-2012. The
849 WASA-SED model also simulates the impact of the small reservoirs on the generated
850 catchment runoff as aforementioned. The WASA-SED results for the storage volumes of the
851 Benguê reservoir were very similar to those produced by the SWAT model presented here,
852 although the WASA-SED model was specifically adjusted only for the Benguê catchment.

853 Furthermore, it can be seen that the model simulated the release from the reservoir during
854 flood events within the calibration and validation periods (Figure 9). Both the durations and
855 the magnitudes of the overflow discharges seem plausible for all reservoirs. According to the
856 specific stage-discharge curves edited for this study the simulated maximum discharge from
857 Poço da Pedra corresponds to a water stage of about 60 cm above the spillway crest. The
858 maximum simulated overflow discharge from Do Coronel would cause the water stage to reach
859 a height of 40 cm above the spillway crest. The maximum discharge from Benguê corresponded
860 to a water stage higher than 2 m above the spillway crest. 2.1 m is given as the maximum water
861 level above the spillway. So, in this case it may be assumed that the model overestimated the
862 outflow. But as the outflow from the spillway represents a dynamic process, depending on
863 hourly flood events, the water stage may be kept constant during a longer time span, leading to
864 higher discharges than the one predicted by the stage-discharge curves, which assume no
865 further inflow to the reservoir. As no information was available regarding the spillway
866 overflow from the reservoirs, no further comments on the plausibility of the outflow
867 hydrographs were done. However, the results were an indication that the filling and emptying
868 processes in reservoirs may be mimicked realistically with the SWAT model even on a daily
869 time step, which was rarely shown before.

870

871 **[Figure 8 is around here]**

872

873 **[Figure 9 is around here]**

874

875 Beyond the results presented for reservoirs, an analysis was also made for the number of
876 days on which the three reservoirs overflowed. These results were taken from analysis of the
877 simulation, counting the days when each reservoir exceeded capacity resulting in spillway
878 overflow during the simulation period (1979 – 2010). These values were compared with the
879 number of spillway overflow days from the state water agency observed data for each reservoir.
880 The results were presented in Table 8. The model greatly overestimated the number of days
881 with spillway overflow, mainly for Poço da Pedra and Benguê. This is an expected result, since
882 the hydrographs of these reservoirs for model simulation had several years reaching their
883 capacities. On the other hand, for Do Coronel the results were very close. A greater number of
884 days of spillway overflow from the reservoirs implies that more water reaches the outlet of the
885 catchment, increasing the simulated streamflow values. This could be clearly seen in 2009,
886 where all reservoirs overflowed and, consequently, the simulated peak flow at the Malhada
887 station was much higher than the observed peak flow. Other years that also had simulated
888 streamflow rates greater than those observed (2006, 2007, 2008 and 2010) coincided with the
889 overflow of the reservoirs having a higher number of days in these years.

890

891 **[Table 8 is around here]**

892

893 Figure 10 depicts the outflow hydrographs for four selected main private dams
894 implemented as reservoirs for the entire simulation period (1979 – 2010). The two main private
895 reservoirs with the largest drainage area and the largest storage volume (No. 46 and No. 146

896 respectively) and the largest main private reservoirs for Poço da Pedra catchment (No. 123)
897 and Benguê catchment (No. 17) were chosen for presentation (see Figure 1), as they had the
898 highest hydrological impact. The diagrams showed that water release from the reservoirs 17,
899 46 and 123 was simulated by the model only in some years, with the spilling lasting only for a
900 couple of days. As presented before, it was expected that such medium-sized reservoirs spill
901 out only in wet years after consecutive strong rain events. These results agree with this field
902 observation. Hence, the spilling behavior seems realistic. With regard to the spillway outflow
903 simulated for these main private reservoirs, the magnitude of the discharges were consistent
904 considering the smaller drainage areas and the spillway widths estimated. Consequently, it may
905 be stated that the estimation of the reservoir capacity and the model parameterization were
906 reasonable. No other information nor observed data was available for these reservoirs.
907 Therefore, the plausibility of the results may not be assessed more specifically.

908 The higher frequency and duration of spilling of reservoir number 146 simulated by the
909 model were due to the fact that the soil type present in that area does not have any cracking
910 potential. Therefore, the soil was saturated faster and more runoff was generated leading to a
911 faster filling of the reservoir. As the spillway outflow magnitudes were consistent to the
912 drainage area and the spillway width and the parametrization was based on the calibration of
913 the volume of Do Coronel reservoir located nearby, it may be assumed that these results, too,
914 were reasonable.

915

916 **[Figure 10 is around here]**

917

918 ***3.3 Impact of the reservoir network on streamflow and reservoir volume*** 919 ***simulations***

920 The influence of reservoirs on the outflow of the catchment was first investigated with the
921 following four scenarios for the whole flow series (1979 – 2010): (i) considering all strategic
922 reservoirs and small reservoirs (reference); (ii) removing all small reservoirs in the
923 hydrological system, but keeping only the strategic reservoirs; (iii) removing all strategic
924 reservoirs but keeping only the small reservoirs; (iv) removing all reservoirs. Table 9 presents
925 a comparison for the model results criteria (PBIAS, NSE and KGE) between the four scenarios.
926 The analysis of the statistical criteria in Table 9 showed that removing strategic reservoirs
927 significantly reduced the PBIAS, which means an increase in the simulated streamflow in the
928 outlet. Also, NSE and KGE decreased. This result is in line with the expectations due to the
929 decrease in retention by removing the reservoirs.

930

931 **[Table 9 is around here]**

932

933 Besides that, to illustrate the results obtained for wet years, the year of 2004 was chosen to
934 show the comparison between the simulations, with the streamflow in the outlet at logarithmic
935 scale (Figure 11). The streamflow hydrograph showed that, during the first increasing limb, the
936 scenarios had a similar slope, but the scenarios (iii) and (iv) reached a higher peak flow.
937 Scenarios (iii) and (iv) do not have strategic reservoirs, therefore water retention was lower in
938 the catchment. After this point, all the scenarios showed similar results. As the differences
939 between scenarios (i) and (ii) and between scenarios (iii) and (iv) were very small, this result
940 also showed that the presence of small reservoirs did not significantly alter the streamflow
941 during the rainy season. The water retention due to small reservoirs in wet years was 2%. The
942 decreasing limb and the recession flow showed the same aspect observed in model calibration,
943 with the end of wet periods to be abrupt, with streamflow going down to zero faster than the
944 observed values, probably due to river-aquifer interaction processes that were not caught by

945 SWAT as aforementioned. This behaviour is also seen in other wetted years, such as 1985 and
946 2009 (not shown here). Therefore, these results indicated that the basin under study is far from
947 reaching its maximum water reserve capacity, especially considering the saturation of small
948 reservoirs.

949 All scenarios overestimate the observed streamflow data, which can be seen more clearly
950 on the cumulative streamflow representation (Figure 11). For the scenarios (i) and (ii), during
951 the intermediate rainy season, the simulated recession flow was higher than the observed one,
952 mainly from 02/2004 to 03/2004. Furthermore, the scenarios (iii) and (iv) reached a higher
953 peak flow at the beginning of the rainy season, due to the absence of the strategic reservoirs.

954

955 **[Figure 11 is around here]**

956

957 To illustrate the results obtained for dry years with low flows, the year of 2003 was chosen
958 to show the comparison between the simulations and the observed data, with the streamflow in
959 the outlet at logarithmic scale (Figure 12). The results were very similar to those obtained for
960 wet years. All scenarios overestimate the observed streamflow data. However, the differences
961 between scenarios (i) and (ii) and between scenarios (iii) and (iv) showed that the presence of
962 small reservoirs is more significant for reducing the cumulative streamflow during a dry year.
963 The water retention due to small reservoirs in dry years was 9%. Other studies have also shown
964 that small reservoirs decrease low flows, with a more intense reduction in dry years (Perrin et
965 al., 2012; Habets et al., 2018).

966

967 **[Figure 12 is around here]**

968

969 Now, modifying the dimensions of the small reservoirs ten times, we found a lower
970 streamflow peak for the estimation with small reservoirs parameters ten times larger than the
971 reference (original parameterization). This result was expected, because with more small
972 reservoirs in the catchment, more water retention is observed, which means less outflow to the
973 Malhada station. Despite this, the comparison of scenario simulations (the absence of small
974 reservoirs, the reference and the larger dimensions of small reservoirs) for peak flow,
975 increasing and decreasing limb were very close, with no considerable differences between the
976 model scenarios for small reservoirs, even in dry years (not shown here).

977 The analysis of the reservoir volumes for the scenarios was carried out by a comparison of
978 the time series of the storage volumes (Figures 13, 14 and 15). The results showed a small
979 difference for the storage volume in the Poço da Pedra reservoir (Figure 13) considering the
980 changes in the dimensions of the small reservoirs. For the Benguê and Do Coronel reservoirs
981 (Figures 14 and 15, respectively), the differences in the storage volume can be observed more
982 clearly between 2002 and 2004, with larger volumes for the "0 times" simulation, which means
983 the absence of small reservoirs, and slightly smaller volumes for the "10 times" simulation.
984 Once again, this was an expected result, because by decreasing the small reservoirs more water
985 can reach the strategic reservoirs, increasing the storage volumes. However, the differences
986 between the simulations were not considerable to conclude for a relevant impact of small
987 reservoirs on those catchments.

988

989 **[Figure 13 is around here]**

990

991 **[Figure 14 is around here]**

992

993 **[Figure 15 is around here]**

994

995 Previous studies suggest a relatively high impact of small reservoirs on the catchment water
996 retention - from 10% to 20% (Araújo and Medeiros, 2013; Peter et al., 2014; Mamede et al.,
997 2018; Habets et al., 2020), while the present model with new representation of small reservoirs
998 in SWAT showed a lower impact on the water inflow for strategic reservoirs (about 2% of
999 water retention in wet years and about 9% in dry years). The study basin has an estimate of 230
1000 reservoirs distributed over a total catchment area of 3,347 km², resulting in 1 reservoir per 14.5
1001 km² (reservoir density). For semi-arid regions, the variability of spatial distribution and density
1002 of small reservoirs varies significantly, between 0 and 4.2 reservoirs per km² (Mady et al.,
1003 2020). In comparison with other dryland regions, the Conceição River Catchment reservoir
1004 density is 25 times bigger than reservoir density in California, USA, as reported by Minear and
1005 Kondolf (2009), for example. Despite the large number of reservoirs in the Upper Jaguaribe
1006 Basin (UJB), where the study area is located, we found a reservoir density 2.5 times smaller
1007 than that of the whole UJB, which is 1 reservoir per 6 km² (Lima Neto et al., 2011). This
1008 indicates that the study area can still be considered to have a high density of reservoirs, although
1009 it has a lower reservoir density than the average of the UJB.

1010 Furthermore, considering the observed data from 1979 to 2010, the main hydrologic fluxes
1011 of the study are: annual precipitation, annual potential evapotranspiration and annual
1012 streamflow of 605 mm, 2,328 mm and 67.8 hm³/year (20.3 mm), respectively. The total
1013 estimated reservoir capacity is 113.1 hm³ (or 33.8 mm), of which 94.0 hm³ (28.1 mm) comes
1014 from three strategic reservoirs. Ponds and main private reservoirs (226) have only 19.1 hm³
1015 (5.7 mm), on average 0.085 hm³ (0.025 mm) per small reservoir. Even increasing the volume
1016 estimates of small reservoirs by ten times, the average volume per area of each small reservoir
1017 (0.25 mm) remains very small in comparison with strategic reservoirs and the aforementioned
1018 hydrologic fluxes. Moreover, as the stream flow are normally concentrated in a few days of the

1019 year in this catchment, the surface runoff has much more volume than the capacity of the small
1020 reservoirs, even for forcing moderate rainfall events.

1021 Although the results obtained in this work represent hydrological aspects of a specific
1022 catchment in the Brazilian semiarid region, the methodology for assessing the impact of small
1023 reservoirs and the discussion of hydrological processes, such as peak flow and non-flow
1024 periods, channel transmission losses, analysis at the beginning and end of the rainy season in
1025 the streamflow gauge station hydrographs and in the storage volume of reservoirs, as well as
1026 the parameterization of the dense network of reservoirs, can also be applied to large-scale
1027 catchments located in other dryland regions. Some examples include semi-arid watersheds in
1028 Australia, United States, Mexico and South Asia, which present similar climate, hydrological
1029 and land-use characteristics.

1030

1031 **4 Conclusions**

1032 In this study, we assessed the impact of small reservoirs on a dryland catchment with a
1033 high-density network of reservoirs and investigated the water routing dynamics and
1034 hydrological processes in the basin. For this purpose, a model was developed to simulate the
1035 catchment streamflow at the outlet, the storage volumes of large reservoirs and the water
1036 balance of lumped small-reservoirs at sub-basin scale. A methodology for the parameterization
1037 of the small reservoirs was developed to represent their integration into the catchment
1038 hydrological modeling and to investigate their influence on the hydrological outputs
1039 (streamflow and reservoir volume storage) of the basin.

1040 The main findings of our work can be described as follows:

- 1041 1. The model proved to be well suited for simulating peak flow in wet years, the non-flow
1042 periods and the rising limb of the hydrograph with high reliability for the streamflow at
1043 the catchment outlet.

- 1044 2. In the strategic reservoirs, wet and dry years were well represented, as well as the
1045 magnitude of spillway overflow of strategic and small reservoirs. On the other hand, the
1046 number of days with spillway overflow showed to be overestimated.
- 1047 3. The proposed model presents an innovative way to represent a dense network of
1048 reservoirs in semi-arid basins in catchment hydrological models. The efforts in the
1049 parameterization and aggregation of ponds and reservoirs proved to be worthwhile,
1050 allowing a more accurate spatial representation of the strategic and small reservoirs in
1051 the SWAT model for high-density networks and improving the analysis of the
1052 hydrological processes and impacts in the basin.
- 1053 4. The presence of small reservoirs decreased the stream flow and storage downstream
1054 reservoir volumes, with only 2% of water retention on average. Increasing the volumes
1055 of small reservoirs along the basin by ten times showed that the small ponds had a low
1056 influence on stream discharge. The catchment under study is far from reaching its
1057 maximum water reserve capacity, especially considering the current density of small
1058 reservoirs. However, in dry years, their impact can reach 9% of water retention, which
1059 may worsen periods of water scarcity in the large reservoirs.

1060 For semi-arid catchments, the reliability of the results for peak flow in wet years, for non-
1061 flow periods and for the rising limb of the hydrograph is very important for the simulation of
1062 the stream flow reaching the large reservoirs and, consequently, for meeting the water demand
1063 at catchment scale. However future improvements should be done in the model for better
1064 representations in recession flow.

1065 Since the results of the present study pointed to a low influence of the network of small
1066 reservoirs on the stream flow and strategic reservoir storages, the small reservoirs in the
1067 catchment might be an option to increase decentralized water access for small rural

1068 communities, without competing with other water uses, such as large and medium-sized city
1069 sanitation demands and irrigation industry, from the strategic reservoirs.

1070 The spatial representation of small reservoirs for a high-density network in the SWAT
1071 model and the results of the cumulative impact of small reservoirs presented in this study
1072 contributed to a better understanding of hydrology in dryland catchments, and can be applied
1073 to catchments in similar climatic and socio-economic environments. Further studies on the
1074 SWAT model in semi-arid regions will evaluate different arrangements for the increase of
1075 small reservoirs in the basin and their impact on reservoir water quality. Such studies should
1076 also be concerned with investigating channel transmission losses and river-aquifer interactions,
1077 based on comparison with additional (intermittent) groundwater data. The coupling of surface
1078 and groundwater models will potentially improve the understanding of dryland hydrology and
1079 integrated water resources management in semi-arid regions.

1080

1081 **Conflict of interest**

1082 There is no conflict of interest.

1083

1084 **Acknowledgements**

1085 We would like to thank the Foundation for Meteorology and Water Resources of the State of Ceará
1086 (FUNCEME) for making available the DEM, the raw information about the landscape properties and
1087 the meteorological time series and the Deutscher Akademischer Austauschdienst (DAAD) for
1088 supporting field work. We also thank the Water Agency of the State of Ceará (COGERH) and the
1089 Secretary of Water Resources of the government of Ceará (SRH) for providing reservoir data. Finally,
1090 we are grateful for the streamflow time series, which were made available by the Brazilian Water
1091 Agency (ANA).

1092

1093 **Funding**

1094 This study was supported by the Foundation for Scientific and Technological Development of the State
1095 of Ceará (FUNCAP) (PNE0112–00042.01.00 / 16), the Brazilian National Council for Scientific and
1096 Technological Development (CNPq) (155814 / 2018–4) and by Deutscher Akademischer
1097 Austauschdienst (DAAD).

1098

1099 **References**

1100 Abouabdillah, A., White, M., Arnold, J.G., De Girolamo, A.M., Oueslati, O., Maataoui, A., Lo
1101 Porto, A., 2014. Evaluation of soil and water conservation measures in a semi-arid river
1102 basin in Tunisia using SWAT. *Soil Use Manag.* 30, 539–549.
1103 <https://doi.org/10.1111/sum.12146>.

1104 AghaKouchak, A., Feldman, D., Hoerling, M., Huxman, T., Lund, J., 2015. Water and climate:
1105 Recognize anthropogenic drought. *Nat.* 2015 5247566 524, 409–411.
1106 <https://doi.org/10.1038/524409a>.

1107 Aigner, D., 2008. *Dresdner Wasserbauliche Mitteilungen Heft 36. Überfälle*. Edited by
1108 Technische Universität Dresden. Dresden. Available online at [http://rcswww.urz.tu-](http://rcswww.urz.tu-dresden.de/~daigner/pdf/ueberf.pdf)
1109 [dresden.de/~daigner/pdf/ueberf.pdf](http://rcswww.urz.tu-dresden.de/~daigner/pdf/ueberf.pdf).

1110 Andaryani, S., Trolle, D., Nikjoo, M.R., Moghadam, M.H.R., Mokhtari, D., 2019. Forecasting
1111 near-future impacts of land use and climate change on the Zilbier river hydrological
1112 regime, northwestern Iran. *Environ. Earth Sci.* 78, 1–14. [https://doi.org/10.1007/s12665-](https://doi.org/10.1007/s12665-019-8193-4)
1113 [019-8193-4](https://doi.org/10.1007/s12665-019-8193-4).

1114 Andrade, C.W.L. de, Montenegro, S.M.G.L., Montenegro, A.A.A., Lima, J.R. de S.,
1115 Srinivasan, R., Jones, C.A., 2019. Soil moisture and discharge modeling in a
1116 representative watershed in northeastern Brazil using SWAT. *Ecohydrol. Hydrobiol.* 19,
1117 238–251. <https://doi.org/10.1016/j.ecohyd.2018.09.002>.

1118 Araújo, J.C., Medeiros, P.H.A., 2013. Impact of Dense Reservoir Networks on Water
1119 Resources in Semiarid Environments. *Australas. J. Water Resour.* 17, 87–100.
1120 <https://doi.org/10.7158/13241583.2013.11465422>.

1121 Arnold, J.G., Moriasi, D.N., Gassman, P.W., Abbaspour, K.C., White, M.J., Srinivasan, R.,
1122 Santhi, C., Harmel, R.D., van Griensven, A., Van Liew, M.W., Kannan, N., Jha, M.K.,
1123 2012. SWAT: Model Use, Calibration, and Validation. *Trans. ASABE* 55, 1491–1508.
1124 <https://doi.org/10.13031/2013.42256>.

1125 Attarod, P., Sadeghi, S.M.M., Pypker, T.G., Bagheri, H., Bagheri, M., Bayramzadeh, V., 2015.
1126 Needle-leaved trees impacts on rainfall interception and canopy storage capacity in an
1127 arid environment. *New For.* 46, 339–355. <https://doi.org/10.1007/s11056-014-9464-2>.

1128 Ayalew, T.B., Krajewski, W.F., Mantilla, R., Wright, D.B., Small, S.J., 2017. Effect of
1129 Spatially Distributed Small Dams on Flood Frequency: Insights from the Soap Creek
1130 Watershed. *J. Hydrol. Eng.* 22, 04017011. [https://doi.org/10.1061/\(ASCE\)HE.1943-](https://doi.org/10.1061/(ASCE)HE.1943-5584.0001513)
1131 [5584.0001513](https://doi.org/10.1061/(ASCE)HE.1943-5584.0001513).

1132 Benites, V.M., Machado, P.O.A., Fidalgo, E.C.C., Coelho, M.R., Madari, B.E., Lima, C.X.,
1133 2006. Funções de Pedotransferência para Estimativa da Densidade dos Solos Brasileiros.
1134 *Boletim de Pesquisa e Desenvolvimento, Ministério da Agricultura, Pecuária e*
1135 *Abastecimento, Empresa Brasileira de Pesquisa Agropecuária.* ISSN: 1678-0892.

1136 Berg, M.D., Popescu, S.C., Wilcox, B.P., Angerer, J.P., Rhodes, E.C., McAlister, J., Fox, W.E.,
1137 2016. Small farm ponds: overlooked features with important impacts on watershed
1138 sediment transport. *JAWRA J. Am. Water Resour. Assoc.* 52, 67–76.
1139 <https://doi.org/10.1111/1752-1688.12369>.

1140 Berhane, G., Gebreyohannes, T., Martens, K., Walraevens, K., 2016. Overview of micro-dam
1141 reservoirs (MDR) in Tigray (northern Ethiopia): Challenges and benefits. *J. African*
1142 *Earth Sci.* 123, 210–222. <https://doi.org/10.1016/J.JAFREARSCI.2016.07.022>.

1143 Bressiani, D.A., Gassman, P.W., Fernandes, J.G., Hamilton, L., Garbossa, P., Srinivasan, R.,
1144 Bonumá, N.B., Mendiondo, E.M., 2015. Review of Soil and Water Assessment Tool
1145 (SWAT) applications in Brazil: challenges and prospects. *Int. J. Agric. Biol. Eng.* 8, 9–
1146 35. <https://doi.org/10.25165/ijabe.v8i3.1765>.

1147 Bronstert, A., de Araújo, J.-C., Batalla, R.J., Costa, A.C., Delgado, J.M., Francke, T., Foerster,
1148 S., Guentner, A., López-Tarazón, J.A., Mamede, G.L., Medeiros, P.H., Mueller, E.,
1149 Vericat, D., 2014. Process-based modelling of erosion, sediment transport and reservoir
1150 siltation in mesoscale semi-arid catchments. *J. Soils Sediments* 2014 1412 14, 2001–
1151 2018. <https://doi.org/10.1007/S11368-014-0994-1>.

1152 Callow, J.N., Smettem, K.R.J., 2009. The effect of farm dams and constructed banks on
1153 hydrologic connectivity and runoff estimation in agricultural landscapes. *Environ.*
1154 *Model. Softw.* 24, 959–968. <https://doi.org/10.1016/j.envsoft.2009.02.003>.

1155 Carluer N., Babut M., Belliard J., Bernez I., Burger-Leenhardt D., Dorioz J.M., Douez O.,
1156 Dufour S., Grimaldi C., Habets F., Le Bissonnais Y., Molénat J., Rollet A.J., Rosset V.,
1157 Sauvage S., Usseglio-Polatera P., Leblanc B., 2016. Expertise scientifique collective sur
1158 l'impact cumulé des retenues. Rapport de synthèse. 82 pp + annexes.

1159 Colares, J.Q.d.S., Feitosa F.A.C., 1998. Diagnóstico do Município de Campos Sales. Edited by
1160 Ministério de Minas e Energia, Serviço Geológico do Brasil. Fortaleza (Programa de
1161 Recenseamento de Fontes de Abastecimento por Água Subterrânea no Estado do Ceará).

1162 Costa, A.C., Bronstert, A., De Araújo, J.C., 2012. A channel transmission losses model for
1163 different dryland rivers. *Hydrol. Earth Syst. Sci.* 16, 1111–1135.
1164 <https://doi.org/10.5194/hess-16-1111-2012>.

1165 Costa, A.C., Foerster, S., de Araújo, J.C., Bronstert, A., 2013. Analysis of channel transmission
1166 losses in a dryland river reach in north-eastern Brazil using streamflow series,

1167 groundwater level series and multi-temporal satellite data. *Hydrol. Process.* 27, 1046–
1168 1060. <https://doi.org/10.1002/hyp.9243>.

1169 Daggupati, P., Pai, N., Ale, S., Douglas-Mankin, K.R., Zeckoski, R.W., Jeong, J., Parajuli,
1170 P.B., Saraswat, D., Youssef, M.A., 2015. A Recommended Calibration and Validation
1171 Strategy for Hydrologic and Water Quality Models. *Trans. ASABE* 58, 1705–1719.
1172 <https://doi.org/10.13031/TRANS.58.10712>.

1173 de Figueiredo, J.V., de Araújo, J.C., Medeiros, P.H.A., Costa, A.C., 2016. Runoff initiation in
1174 a preserved semiarid Caatinga small watershed, Northeastern Brazil. *Hydrol. Process.*
1175 30, 2390–2400. <https://doi.org/10.1002/hyp.10801>.

1176 Eudoro, W.S., 2009. *Caderno Regional da Sub-bacia do Alto Jaguaribe*. Edited by Assembleia
1177 Legislativa do Estado, Conselho de Altos Estudos e Assuntos Estratégicos. INESP.
1178 Fortaleza, CE (Coleção Cadernos Regionais do Pacto das Águas, Volume 5).

1179 Feitosa, F.A.C., 1998. *Diagnóstico do Município de Aiuaba*. Edited by Ministério de Minas e
1180 Energia, Serviço Geológico do Brasil. Fortaleza (Programa de Recenseamento de Fontes
1181 de Abastecimento por Água Subterrânea no Estado do Ceará).

1182 Feitosa, F.A.C.; Oliveira, F.V.C. de, 1998. *Diagnóstico do Município de Salitre*. Edited by
1183 Ministério de Minas e Energia, Serviço Geológico do Brasil. Fortaleza (Programa de
1184 Recenseamento de Fontes de Abastecimento por Água Subterrânea no Estado do Ceará).

1185 Fowe, T., Karambiri, H., Paturel, J.E., Poussin, J.C., Cecchi, P., 2015. Water balance of small
1186 reservoirs in the volta basin: A case study of boura reservoir in burkina faso. *Agric. Water*
1187 *Manag.* 152, 99–109. <https://doi.org/10.1016/j.agwat.2015.01.006>.

1188 Fowler, K., Morden, R., Lowe, L., Nathan, R., 2016. Advances in assessing the impact of
1189 hillside farm dams on streamflow. <https://doi.org/10.1080/13241583.2015.1116182> 19,
1190 96–108. <https://doi.org/10.1080/13241583.2015.1116182>.

1191 Gatto, L.C.S., 1999. Diagnóstico Ambiental da Bacia do Rio Jaguaribe. Diretrizes Gerais para
1192 a Ordenação Territorial. 1st ed. Edited by Função Instituto Brasileiro de Geografia e
1193 Estatística, IBGE, Diretoria Geociências. Ministério de Planejamento e Orçamento.
1194 Salvador (DIGEO, 1).

1195 Ghoraba, S.M., 2015. Hydrological modeling of the Simly Dam watershed (Pakistan) using
1196 GIS and SWAT model. Alexandria Eng. J. 54, 583–594.
1197 <https://doi.org/10.1016/j.aej.2015.05.018>.

1198 Gudmundsson, L., Bremnes, J.B., Haugen, J.E., Engen-Skaugen, T., 2012. Technical Note:
1199 Downscaling RCM precipitation to the station scale using statistical transformations
1200 – A comparison of methods. Hydrol. Earth Syst. Sci. 16, 3383–3390.
1201 <https://doi.org/10.5194/hess-16-3383-2012>.

1202 Güntner, A., 2002. Large-Scale Hydrological Modelling in the Semi-Arid North-East of Brazil.
1203 Dissertation. University of Potsdam, Potsdam. Department of Geoecology.

1204 Güntner, A., Krol, M.S., Araújo, J.C. De, Bronstert, A., 2004. Simple water balance modelling
1205 of surface reservoir systems in a large data-scarce semiarid region / Modélisation simple
1206 du bilan hydrologique de systèmes de réservoirs de surface dans une grande région semi-
1207 aride pauvre en données. Hydrol. Sci. J. 49. <https://doi.org/10.1623/hysj.49.5.901.55139>.

1208 Gutiérrez, A.P.A., Engle, N.L., De Nys, E., Molejón, C., Martins, E.S., 2014. Drought
1209 preparedness in Brazil. Weather Clim. Extrem. 3, 95–106.
1210 <https://doi.org/10.1016/j.wace.2013.12.001>.

1211 Habets, F., Molénat, J., Carluer, N., Douez, O., Leenhardt, D., 2018. The cumulative impacts
1212 of small reservoirs on hydrology: A review. Sci. Total Environ. 643, 850–867.
1213 <https://doi.org/10.1016/J.SCITOTENV.2018.06.188>.

- 1214 Hughes, D.A., Mantel, S.K., 2010. Estimating the uncertainty in simulating the impacts of
1215 small farm dams on streamflow regimes in South Africa. *Hydrol. Sci. J.* 55, 578–592.
1216 <https://doi.org/10.1080/02626667.2010.484903>
- 1217 IBGE – Instituto Brasileiro de Geografia e Estatística, 2011. Censo demográfico 2010:
1218 Características da população e dos domicílios – resultados do universo. Rio de Janeiro.
1219 Available online at: [https://sidra.ibge.gov.br/pesquisa/censo-demografico/demografico-](https://sidra.ibge.gov.br/pesquisa/censo-demografico/demografico-2010/universo-caracteristicas-da-populacao-e-dos-domicilios)
1220 [2010/universo-caracteristicas-da-populacao-e-dos-domicilios](https://sidra.ibge.gov.br/pesquisa/censo-demografico/demografico-2010/universo-caracteristicas-da-populacao-e-dos-domicilios)
- 1221 Jacomine, P.K.T., Almeida, J.C., Medeiros, L.A.R., 1973. Levantamento Exploratório -
1222 Reconhecimento de Solos do Estado do Ceará. Edited by Divisao de Pesquisa
1223 Pedológica, Divisao de Agrologia. Ministério da Agricultura, Ministério do Interior.
1224 Recife (Convênio de Mapeamento de Solos, 1).
- 1225 Jajarmizadeh, M., Sidek, L.M., Harun, S., Salarpour, M., 2017. Optimal Calibration and
1226 Uncertainty Analysis of SWAT for an Arid Climate:
1227 <https://doi.org/10.1177/1178622117731792>.
- 1228 Kim, K.B., Kwon, H.H., Han, D., 2018. Exploration of warm-up period in conceptual
1229 hydrological modelling. *J. Hydrol.* 556, 194–210.
1230 <https://doi.org/10.1016/J.JHYDROL.2017.11.015>.
- 1231 Lam, K.C., Bryant, R.G., Wainright, J., 2015. Application of spatial interpolation method for
1232 estimating the spatial variability of rainfall in Semiarid New Mexico, USA. *Mediterr. J.*
1233 *Soc. Sci.* 6, 108–116. <https://doi.org/10.5901/mjss.2015.v6n4s3p108>.
- 1234 Lima Neto, I.E., Wiegand, M.C., de Araújo, J.C., 2011. Sediment redistribution due to a dense
1235 reservoir network in a large semi-arid Brazilian basin. *Hydrol. Sci. J.* 56, 319–333.
1236 <https://doi.org/10.1080/02626667.2011.553616>.

1237 Liu, Y., Yang, W., Yu, Z., Lung, I., Yarotski, J., Elliott, J., Tiessen, K., 2014. Assessing Effects
1238 of Small Dams on Stream Flow and Water Quality in an Agricultural Watershed. *J.*
1239 *Hydrol. Eng.* 19, 05014015. [https://doi.org/10.1061/\(ASCE\)HE.1943-5584.0001005](https://doi.org/10.1061/(ASCE)HE.1943-5584.0001005).

1240 Luo, K., Tao, F., Deng, X., Moiwo, J.P., 2016. Changes in potential evapotranspiration and
1241 surface runoff in 1981-2010 and the driving factors in Upper Heihe River Basin in
1242 Northwest China. *Hydrol. Process.* 31, 90–103. <https://doi.org/10.1002/hyp.10974>.

1243 Mady, B., Lehmann, P., Gorelick, S.M., Or, D., 2020. Distribution of small seasonal reservoirs
1244 in semi-arid regions and associated evaporative losses. *Environ. Res. Commun.* 2,
1245 061002. <https://doi.org/10.1088/2515-7620/ab92af>.

1246 Mallakpour, I., Sadegh, M., Aghakouchak, A., 2018. A new normal for streamflow in
1247 California in a warming climate: Wetter wet seasons and drier dry seasons. *J. Hydrol.*
1248 567, 203–211. <https://doi.org/10.1016/j.jhydrol.2018.10.023>.

1249 Malveira, V.T.C., Araújo, J.C. de, Güntner, A., 2012. Hydrological Impact of a High-Density
1250 Reservoir Network in Semiarid Northeastern Brazil. *J. Hydrol. Eng.* 17, 109–117.
1251 [https://doi.org/10.1061/\(asce\)he.1943-5584.0000404](https://doi.org/10.1061/(asce)he.1943-5584.0000404).

1252 Mamede, G.L., Araújo, N.A.M., Schneider, C.M., De Araújo, J.C., Herrmann, H.J., 2012.
1253 Overspill avalanching in a dense reservoir network. *Proc. Natl. Acad. Sci. U. S. A.* 109,
1254 7191–7195. <https://doi.org/10.1073/pnas.1200398109>.

1255 Mamede, G.L., Guentner, A., Medeiros, P.H.A., de Araújo, J.C., Bronstert, A., 2018. Modeling
1256 the Effect of Multiple Reservoirs on Water and Sediment Dynamics in a Semiarid
1257 Catchment in Brazil. *J. Hydrol. Eng.* 23, 05018020.
1258 [https://doi.org/10.1061/\(asce\)he.1943-5584.0001701](https://doi.org/10.1061/(asce)he.1943-5584.0001701).

1259 Maraun, D., 2013. Bias correction, quantile mapping, and downscaling: Revisiting the inflation
1260 issue. *J. Clim.* 26, 2137–2143. <https://doi.org/10.1175/JCLI-D-12-00821.1>.

- 1261 Mendoza, J.A.C., Alcazar, T.A.C., Medina, S.A.Z., 2021. Calibration and Uncertainty Analysis
1262 for Modelling Runoff in the Tambo River Basin, Peru, Using Sequential Uncertainty
1263 Fitting Ver-2 (SUFI-2) Algorithm. <https://doi.org/10.1177/1178622120988707>.
- 1264 Mengistu, A.G., van Rensburg, L.D., Woyessa, Y.E., 2019. Techniques for calibration and
1265 validation of SWAT model in data scarce arid and semi-arid catchments in South Africa.
1266 J. Hydrol. Reg. Stud. 25, 100621. <https://doi.org/10.1016/J.EJRH.2019.100621>.
- 1267 Minear, J.T., Kondolf, G.M., 2009. Estimating reservoir sedimentation rates at large spatial
1268 and temporal scales: A case study of California. Water Resour. Res. 45.
1269 <https://doi.org/10.1029/2007WR006703>.
- 1270 Molina-Navarro, E., Hallack-Alegría, M., Martínez-Pérez, S., Ramírez-Hernández, J.,
1271 Mungaray-Moctezuma, A., Sastre-Merlín, A., 2016. Hydrological modeling and climate
1272 change impacts in an agricultural semiarid region. Case study: Guadalupe River basin,
1273 Mexico. Agric. Water Manag. 175, 29–42. <https://doi.org/10.1016/j.agwat.2015.10.029>.
- 1274 Molle, F., 1989. Perdas por Evaporação e Infiltração em Pequenos Açudes. 2nd ed. Edited by
1275 Superintendência do Desenvolvimento do Nordeste. SUDENE/ORSTOM (TAPI).
1276 Recife, PE (Série Hidrologia, 25). Available online at
1277 [http://horizon.documentation.ird.fr/exldoc/pleins_textes/pleins_textes_7/b_fdi_03_01/3](http://horizon.documentation.ird.fr/exldoc/pleins_textes/pleins_textes_7/b_fdi_03_01/33854.pdf)
1278 [3854.pdf](http://horizon.documentation.ird.fr/exldoc/pleins_textes/pleins_textes_7/b_fdi_03_01/33854.pdf).
- 1279 Molle, F., 1994. Geometria Dos Pequenos Açudes. 2nd ed. Edited by Superintendência do
1280 Desenvolvimento do Nordeste. SUDENE/ORSTOM (TAPI). Recife, PE (Série
1281 Hidrologia, 29). Available online at [http://horizon.documentation.ird.fr/exl-](http://horizon.documentation.ird.fr/exl-doc/pleins_textes/pleins_textes_7/divers2/010033411.pdf)
1282 [doc/pleins_textes/pleins_textes_7/divers2/010033411.pdf](http://horizon.documentation.ird.fr/exl-doc/pleins_textes/pleins_textes_7/divers2/010033411.pdf).
- 1283 Nascimento, A.T.P. do, Cavalcanti, N.H.M., Castro, B.P.L. de, Medeiros, P.H.A., 2019.
1284 Decentralized water supply by reservoir network reduces power demand for water

1285 distribution in a semi-arid basin. *Hydrol. Sci. J.* 64, 80–91.
1286 <https://doi.org/10.1080/02626667.2019.1566728>.

1287 Nathan, R., Jordan, P., Morden, R., 2005. Assessing the impact of farm dams on streamflows,
1288 Part I: Development of simulation tools. *Australas. J. Water Resour.* 9, 1–12.
1289 <https://doi.org/10.1080/13241583.2005.11465259>.

1290 Nathan, R., Lowe, L., 2012. The Hydrologic Impacts of Farm Dams. *Australas J. Water*
1291 *Resour.* 16:1, 75-83. <https://doi.org/10.7158/13241583.2012.11465405>

1292 Neal, B., Nathan, R.J., Schreider, S., Jakeman, A.J., 2002. Identifying the Separate Impact of
1293 Farm Dams and Land Use Changes on Catchment Yield. *Australas. J. Water Resour.* 5,
1294 165–176. <https://doi.org/10.1080/13241583.2002.11465202>.

1295 Neitsch, S.L., Arnold, J.G., Kiniry, J.R., Williams J.R., 2009. Soil and Water Assessment Tool.
1296 Theoretical Documentation. Version 2009. Edited by Texas Water Resource Institute:
1297 Grassland, Soil and Water Research Laboratory - Agricultural Research Service,
1298 Blackland Research Center - Texas AgriLife Research. Texas A&M University System.
1299 College Station, Texas (Texas Water Resources Institute Technical Report, 406).
1300 Available online at <http://swat.tamu.edu/media/99192/swat2009-theory.pdf>.

1301 Nguyen, H.H., Recknagel, F., Meyer, W., Frizenschaf, J., 2017. Analysing the Effects of Forest
1302 Cover and Irrigation Farm Dams on Streamflows of Water-Scarce Catchments in South
1303 Australia through the SWAT Model. *Water* 2017, Vol. 9, Page 33 9, 33.
1304 <https://doi.org/10.3390/W9010033>.

1305 Nguyen, V., Dietrich, J., Uniyal, B., Tran, D., 2018. Verification and Correction of the
1306 Hydrologic Routing in the Soil and Water Assessment Tool. *Water* 10, 1419.
1307 <https://doi.org/10.3390/w10101419>.

1308 Oliveira, L.B., Ribeiro, M.R., Jacomine, P.K.T., Rodrigues, J.J. V., Marques, F.A., 2002.
1309 Funções de pedotransferência para predição da umidade retida a potenciais específicos

1310 em solos do estado de Pernambuco. Rev. Bras. Ciência do Solo 26, 315–323.
1311 <https://doi.org/10.1590/s0100-06832002000200004>.

1312 Paredes-Beltran, B., Sordo-Ward, A., Garrote, L., 2021. Dataset of Georeferenced Dams in
1313 South America (DDSA). Earth Syst. Sci. Data 13, 213–229.
1314 <https://doi.org/10.5194/ESSD-13-213-2021>.

1315 Pereira, B.S., 2017. Estimativa de Volumes de Reservatórios de Região Semiárida com Alta
1316 Densidade de Resevatórios por Sensoriamento Remoto. Dissertation. Instituto Federal de
1317 Educação, Ciência e Tecnologia do Ceará, Fortaleza, CE. Departamento de
1318 Planejamento, Orçamento e Gestão.

1319 Perrin, J., Ferrant, S., Massuel, S., Dewandel, B., Maréchal, J.C., Aulong, S., Ahmed, S., 2012.
1320 Assessing water availability in a semi-arid watershed of southern India using a semi-
1321 distributed model. J. Hydrol. 460–461, 143–155.
1322 <https://doi.org/10.1016/J.JHYDROL.2012.07.002>.

1323 Peter, S.J., de Araújo, J.C., Araújo, N.A.M., Herrmann, H.J., 2014. Flood avalanches in a
1324 semiarid basin with a dense reservoir network. J. Hydrol. 512, 408–420.
1325 <https://doi.org/10.1016/j.jhydrol.2014.03.001>.

1326 Pinheiro, F.D., 2004. Açudagem particular em cooperação no Ceará, Série conViver, 732 p.
1327 Departamento Nacional de Obras Contra a Seca (DNOCS).

1328 Post, D.F., Fimbres, A., Matthias, A.D., Sano, E.E., Accioly, L., Batchily, A.K., Ferreira, L.G.,
1329 2000. Predicting Soil Albedo from Soil Color and Spectral Reflectance Data. Soil Sci.
1330 Soc. Am. J. 64, 1027–1034. <https://doi.org/10.2136/sssaj2000.6431027x>.

1331 Rödiger, T., Geyer, S., Mallast, U., Merz, R., Krause, P., Fischer, C., Siebert, C., 2014. Multi-
1332 response calibration of a conceptual hydrological model in the semiarid catchment of
1333 Wadi al Arab, Jordan. J. Hydrol. 509, 193–206.
1334 <https://doi.org/10.1016/J.JHYDROL.2013.11.026>.

- 1335 Samimi, M., Mirchi, A., Moriasi, D., Ahn, S., Alian, S., Taghvaeian, S., Sheng, Z., 2020.
1336 Modeling arid/semi-arid irrigated agricultural watersheds with SWAT: Applications,
1337 challenges, and solution strategies. *J. Hydrol.*
1338 <https://doi.org/10.1016/j.jhydrol.2020.125418>
- 1339 Santos, C., Almeida, C., Ramos, T., Rocha, F., Oliveira, R., Neves, R., 2018. Using a
1340 Hierarchical Approach to Calibrate SWAT and Predict the Semi-Arid Hydrologic
1341 Regime of Northeastern Brazil. *Water* 10, 1137. <https://doi.org/10.3390/w10091137>.
- 1342 Secretaria dos Recursos Hídricos (2008): Sistema de Informações dos Recursos Hídricos do
1343 Ceará. Edited by SEINFRA/SRH. Fortaleza. Available online at
1344 <http://atlas.srh.ce.gov.br/>, checked on 2/15/2021.
- 1345 Secretaria Executiva do CSBHAIJ (no date): Comitê da sub-bacia hidrografica do Alto
1346 Jaguaribe. Edited by COGERH - Gerência da Bacia do Alto Jaguaribe. Iguatu - CE.
1347 Available online at [http://www.csbhaj.com.br/comissoesgestoras/comissao-gestora-do-](http://www.csbhaj.com.br/comissoesgestoras/comissao-gestora-do-acude-bengue/?pagina=regimento)
1348 [acude-bengue/?pagina=regimento](http://www.csbhaj.com.br/comissoesgestoras/comissao-gestora-do-acude-bengue/?pagina=regimento), checked on 2/15/2021.
- 1349 Schreider, S.Y., Jakeman, A.J., Letcher, R.A., Nathan, R.J., Neal, B.P., Beavis, S.G., 2002.
1350 Detecting changes in streamflow response to changes in non-climatic catchment
1351 conditions: Farm dam development in the Murray-Darling basin, Australia. *J. Hydrol.*
1352 262, 84–98. [https://doi.org/10.1016/S0022-1694\(02\)00023-9](https://doi.org/10.1016/S0022-1694(02)00023-9).
- 1353 Silva, F.J.A., Araújo, A.L., Souza, R.O., 2007. Águas subterrâneas no Ceará - poços instalados
1354 e salinidade. In *Revista Tecnológica Fortaleza (UNIFOR)* 28 (2), pp. 136–159.
- 1355 Simmers, I., 2003. Understanding water in a dry environment. Hydrological processes in arid
1356 and semi-arid zones. Editor, Ian Simmers. Lisse, Abingdon: A.A. Balkema (International
1357 contributions to hydrogeology, 23).
- 1358 Siqueira, M.S., de Alcântara, H.M., Ribeiro, G.N., Medeiros, P.C., Afonso, J.P.S.D., de
1359 Medeiros, A.C., Maracajá, P.B., 2016. Influence of the scale effect on the sediment yield

1360 in not instrumented basins in the semiarid zone. *Revista Brasileira de Gestão Ambiental*,
1361 v. 11, n.01, p.99 – 105.

1362 Sukhbaatar, C., Sajjad, R.U., Luntun, J., Yu, S.-H., Lee, C.-H., 2017. Climate Change Impact
1363 on the Tuul River Flow in a Semiarid Region in Mongolia. *Water Environ. Res.* 89, 527–
1364 538. <https://doi.org/10.2175/106143016X14798353399223>.

1365 Sun, L., Yang, L., Hao, L., Fang, D., Jin, K., Huang, X., 2017. Hydrological Effects of
1366 Vegetation Cover Degradation and Environmental Implications in a Semiarid Temperate
1367 Steppe, China. *Sustainability* 9, 281. <https://doi.org/10.3390/su9020281>.

1368 Tomasella, J., Hodnett, M.G., 1997. Estimating unsaturated hydraulic conductivity of Brazilian
1369 soils using soil-water retention data. *Soil Science*, 162(10), 703-712.

1370 Uniyal, B., Dietrich, J., Vu, N.Q., Jha, M.K., Arumí, J.L., 2019. Simulation of regional
1371 irrigation requirement with SWAT in different agro-climatic zones driven by observed
1372 climate and two reanalysis datasets. *Sci. Total Environ.* 649, 846–865.
1373 <https://doi.org/10.1016/j.scitotenv.2018.08.248>.

1374 Yaeger, M.A., Reba, M.L., Massey, J.H., Adviento-Borbe, M.A.A., 2017. On-Farm Irrigation
1375 Reservoirs in Two Arkansas Critical Groundwater Regions: A Comparative Inventory.
1376 *Appl. Eng. Agric.* 33, 869–878. <https://doi.org/10.13031/AEA.12352>.

1377 Yao, J., Liu, H., Huang, J., Gao, Z., Wang, G., Li, D., Yu, H., Chen, X., 2020. Accelerated
1378 dryland expansion regulates future variability in dryland gross primary production. *Nat.*
1379 *Commun.* 2020 111 11, 1–10. <https://doi.org/10.1038/s41467-020-15515-2>.

1380 Zettam, A., Taleb, A., Sauvage, S., Boithias, L., Belaidi, N., Sánchez-Pérez, J., 2017.
1381 Modelling Hydrology and Sediment Transport in a Semi-Arid and Anthropized
1382 Catchment Using the SWAT Model: The Case of the Tafna River (Northwest Algeria).
1383 *Water* 9, 216. <https://doi.org/10.3390/w9030216>.

- 1384 Zhang, C., Peng, Y., Chu, J., Shoemaker, C.A., Zhang, A., 2012. Integrated hydrological
1385 modelling of small-and medium-sized water storages with application to the upper
1386 fengman reservoir basin of China. *Hydrol. Earth Syst. Sci.* 16, 4033–4047.
1387 <https://doi.org/10.5194/hess-16-4033-2012>.
- 1388 Zhang, S., Foerster, S., Medeiros, P., de Araújo, J.C., Motagh, M., Waske, B., 2016.
1389 Bathymetric survey of water reservoirs in north-eastern Brazil based on TanDEM-X
1390 satellite data. *Sci. Total Environ.* 571, 575–593.
1391 <https://doi.org/10.1016/j.scitotenv.2016.07.0>
- 1392 Zhang, Z., Liu, J., Huang, J., 2020. Hydrologic impacts of cascade dams in a small headwater
1393 watershed under climate variability. *J. Hydrol.* 590, 125426.
1394 <https://doi.org/10.1016/J.JHYDROL.2020.125426>.

Figure captions

Figure 1. Location of the study catchment with the main rivers and reservoirs. The numbers 17 and 123 represent the largest main private reservoirs for Benguê catchment and Poço da Pedra catchment, respectively. The numbers 46 and 146 represent the two main private reservoirs with the largest drainage area and the largest storage volume, respectively.

Figure 2. Schematic illustration of a sub-basin containing two small reservoirs configured in a cascade (left) and a parallel (right) arrangement. DA_{tot} : drainage area of the aggregated pond defining the total drainage fraction of the sub-basin; R_d/R_1 (red squares): downstream/first reservoir; R_u/R_2 (red squares): upstream/second reservoir; DA_d/DA_1 (not hatched): drainage area of downstream/first reservoir; DA_u/DA_2 (hatched in grey): drainage area of upstream/second reservoir; Blue line: river reaches.

Figure 3. Excess volumes corresponding to certain water stages (0.01, 0.05, 0.10, 0.25, 0.50, 0.75 and 1.00 m) above the spillway crest plotted against calculated daily released volume with fitted straight line for Poço da Pedra (top left), Do Coronel (top right), Benguê (bottom left) and Mamoeiro (bottom right) Reservoir.

Figure 4. Flowchart of methods applied in the representation of reservoirs in the SWAT model and in the approaches to impact assessment of small reservoirs in the catchment.

Figure 5. Comparison of observed and simulated daily discharges at Malhada gauging station for: (a) calibration in 1981 – 1995; (b) validation in 1986 – 2010; (c) calibration in 1986 – 2010; (d) validation in 1981 – 1995.

Figure 6. Comparison of observed and simulated log flow duration curves for: (a) calibration in 1981 – 1995; (b) validation in 1986 – 2010; (c) calibration in 1986 – 2010; (d) validation in 1981 – 1995.

Figure 7. Comparison of observed and simulated hydrograph for daily discharges at Malhada gauging station for: (a) calibration year of 1985; (b) validation year of 2004; (c) calibration year of 2004; (d) validation year of 1985.

Figure 8. Comparison of observed by state water agency and simulated by SWAT daily storage volumes in the three strategic reservoirs for the calibration and validation periods: (a) Poço da Pedra (storage capacity 52 hm³, simulation 1986 - 2010) (b) Benguê (storage capacity 19.56 hm³, simulation 2000 - 2010), (c) Do Coronel (storage capacity 1.77 hm³, simulation 2004 - 2010).

Figure 9. Hydrographs of released discharge for simulated outflow over the spillway of the three strategic reservoirs for model simulations: (a) Poço da Pedra – 2004; (b) Poço da Pedra – 1986; (c) Benguê – 2004; (d) Benguê – 2009; (e) Do Coronel – 2004; (f) Do Coronel – 2009.

Figure 10. Hydrographs for simulated daily discharges released from the private reservoirs No. 17 (a), No. 123 (b), No. 46 (c) and No. 146 (d) via spillway for the years 2003-2010.

Fig. 11. Hydrographs and cumulative stream flow at Malhada station showing observed values and 4 scenarios of reservoirs during the year of 2004: scenario (i) considering all strategic reservoirs and small reservoirs (reference); (ii) removing all small reservoirs in the hydrological system, but keeping only the strategic reservoirs; (iii) removing all strategic reservoirs but keeping only the small reservoirs; (iv) removing all reservoirs.

Fig. 12. Hydrographs and cumulative stream flow at Malhada station showing observed values and 4 scenarios of reservoirs during the year of 2003: scenario (i) considering all strategic reservoirs and small reservoirs (reference); (ii) removing all small reservoirs in the hydrological system, but keeping only the strategic reservoirs; (iii) removing all strategic reservoirs but keeping only the small reservoirs; (iv) removing all reservoirs.

Figure 13. Comparison for storage volumes in Poço da Pedra (2000 – 2010) with modifications in the dimensions of the small reservoirs in 0 and 10 times. “0 times” means the total absence of small reservoirs. “10 times” means a ten times increase in the parameters that represent the volumes of these small reservoirs. Model reference means the original parameterization.

Figure 14. Comparison for storage volumes in Benguê (2000 – 2010) with modifications in the dimensions of the small reservoirs in 0 and 10 times. “0 times” means the total absence of small reservoirs. “10 times” means a ten times increase in the parameters that represent the volumes of these small reservoirs. Model reference means the original parameterization.

Figure 15. Comparison for storage volumes in Do Coronel (2000 – 2010) with modifications in the dimensions of the small reservoirs in 0 and 10 times. “0 times” means the total absence of small reservoirs. “10 times” means a ten times increase in the parameters that represent the volumes of these small reservoirs. Model reference means the original parameterization.

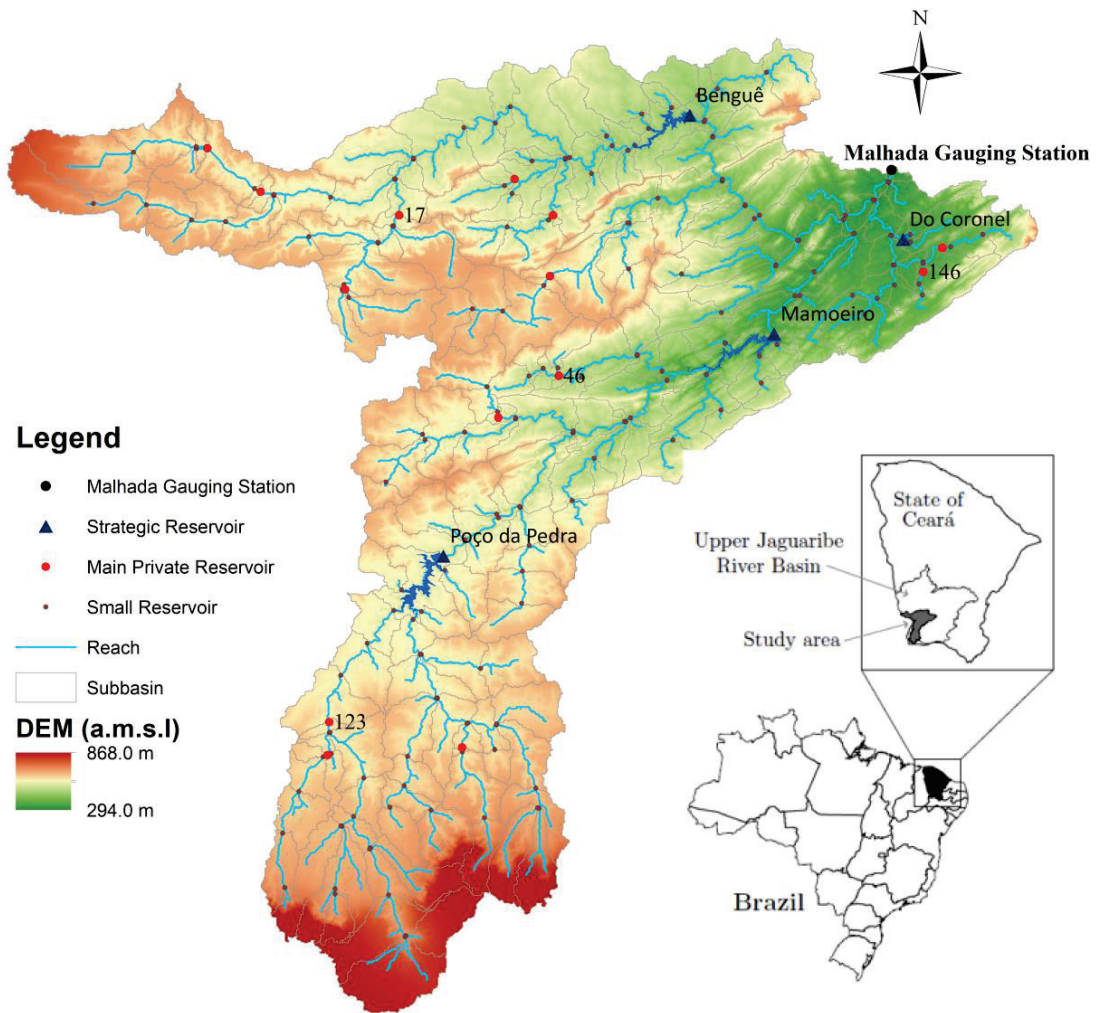


Figure 1 Location of the study catchment with the main rivers and reservoirs. The numbers 17 and 123 represent the largest main private reservoirs for Benguê catchment and Poço da Pedra catchment, respectively. The numbers 46 and 146 represent the two main private reservoirs with the largest drainage area and the largest storage volume, respectively.

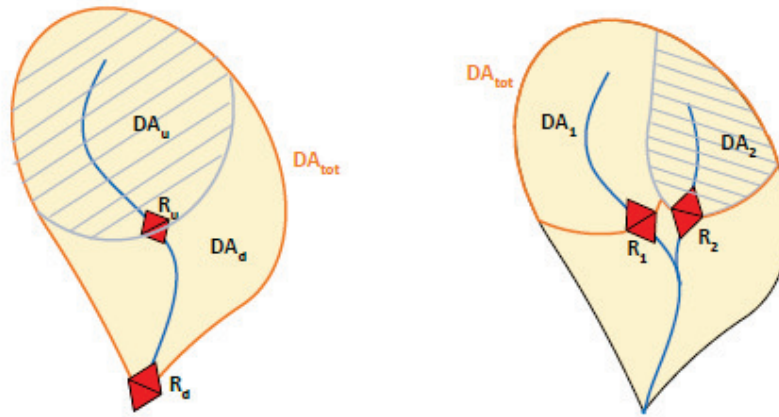


Figure 2 Schematic illustration of a sub-basin containing two small reservoirs configured in a cascade (left) and a parallel (right) arrangement. DA_{tot} : drainage area of the aggregated pond defining the total drainage fraction of the sub-basin; R_d/R_1 (red squares): downstream/first reservoir; R_u/R_2 (red squares): upstream/second reservoir; DA_d/DA_1 (not hatched): drainage area of downstream/first reservoir; DA_u/DA_2 (hatched in grey): drainage area of upstream/second reservoir; Blue line: river reaches.

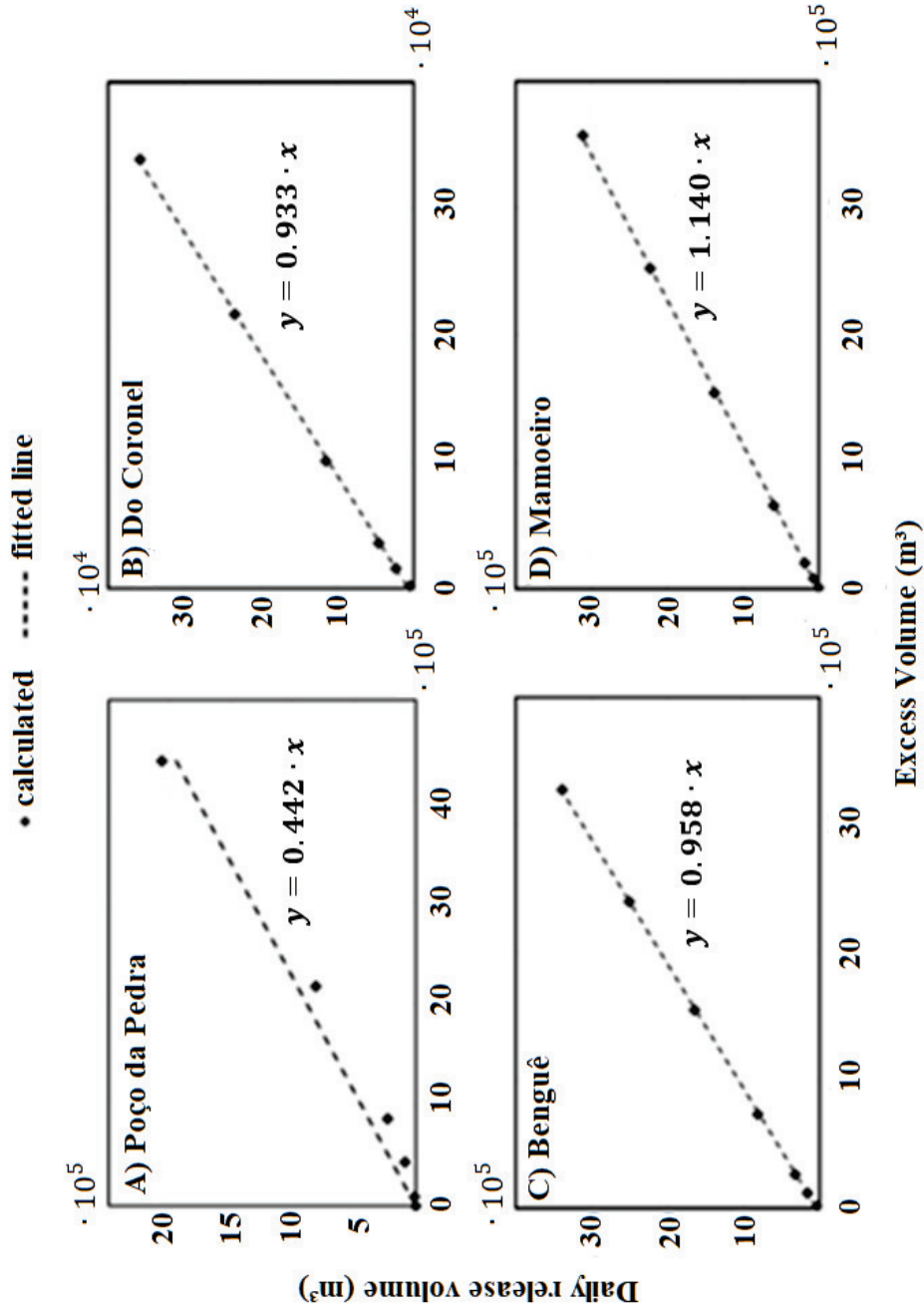
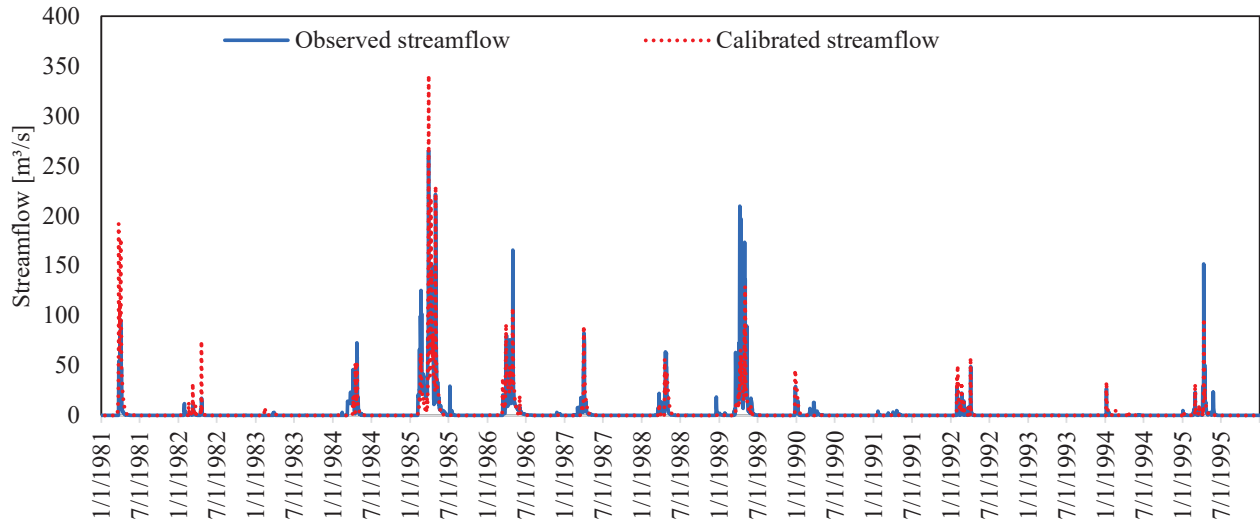


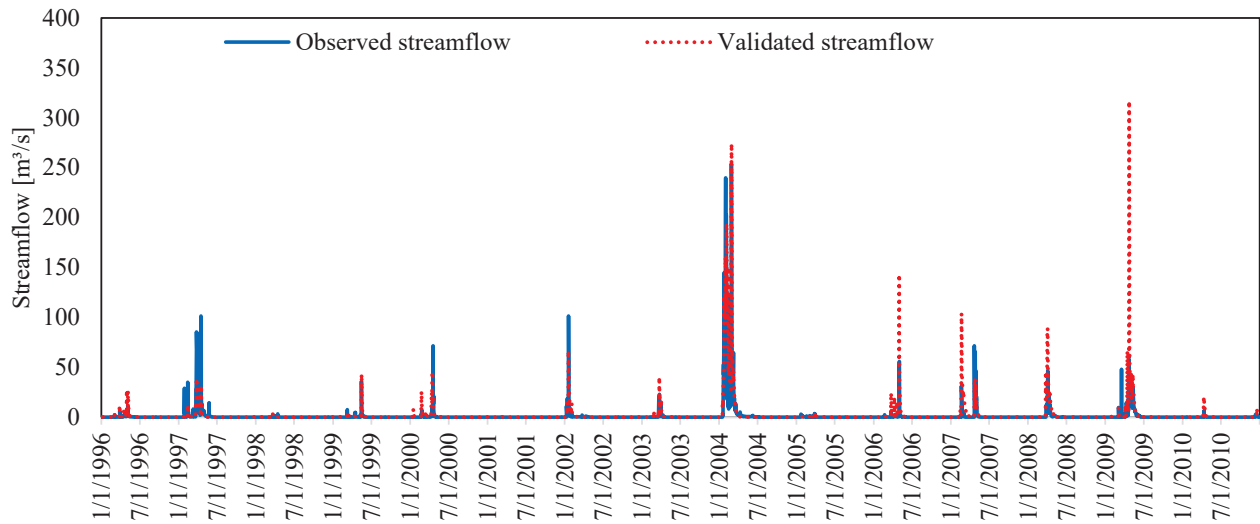
Figure 3 Excess volumes corresponding to certain water stages (0.01, 0.05, 0.10, 0.25, 0.50, 0.75 and 1.00 m) above the spillway crest plotted against calculated daily released volume with fitted straight line for Poço da Pedra (top left), Do Coronel (top right), Benguê (bottom left) and Mamoeiro (bottom right) Reservoir.

Figure 4 Flowchart of methods applied in the representation of reservoirs in the SWAT model and in the approaches to impact assessment of small reservoirs in the catchment.

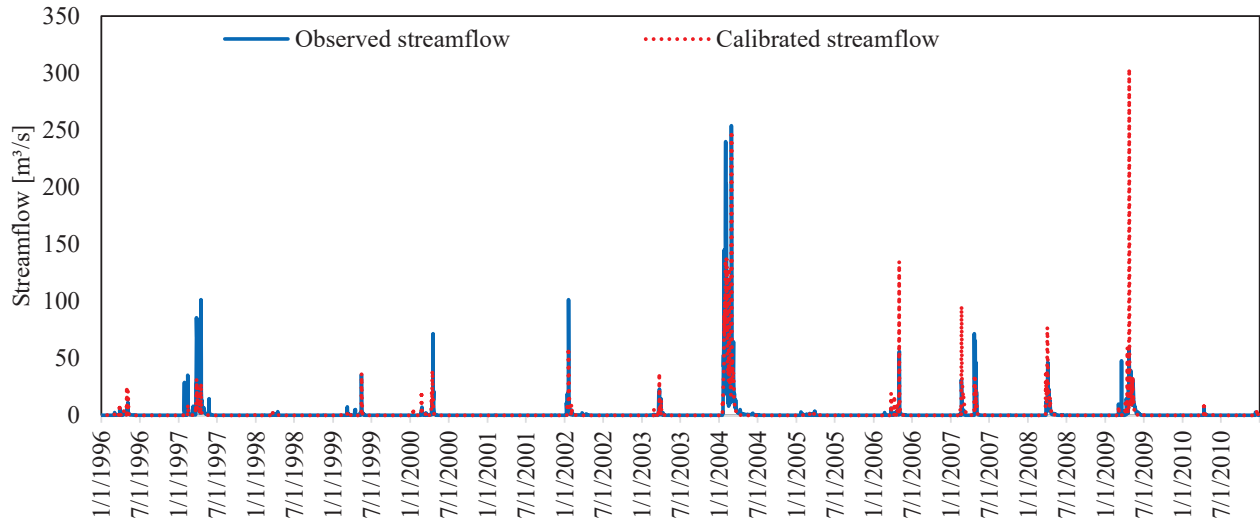
(a) Hydrograph for Malhada gauging station for the calibration period of 1981 - 1995



(b) Hydrograph for Malhada gauging station for the validation period of 1996 - 2010



(c) Hydrograph for Malhada gauging station for the calibration period of 1996 - 2010



(d) Hydrograph for Malhada gauging station for the validation period of 1981 - 1995

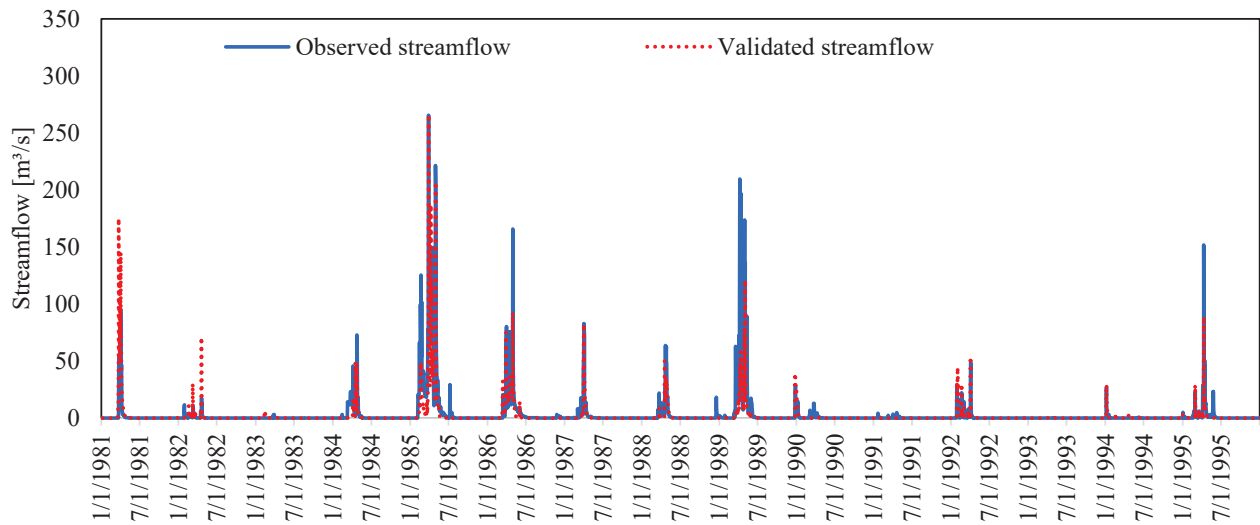


Figure 5 Comparison of observed and simulated daily discharges at Malhada gauging station for: (a) calibration in 1981 – 1995; (b) validation in 1986 – 2010; (c) calibration in 1986 – 2010; (d) validation in 1981 – 1995.

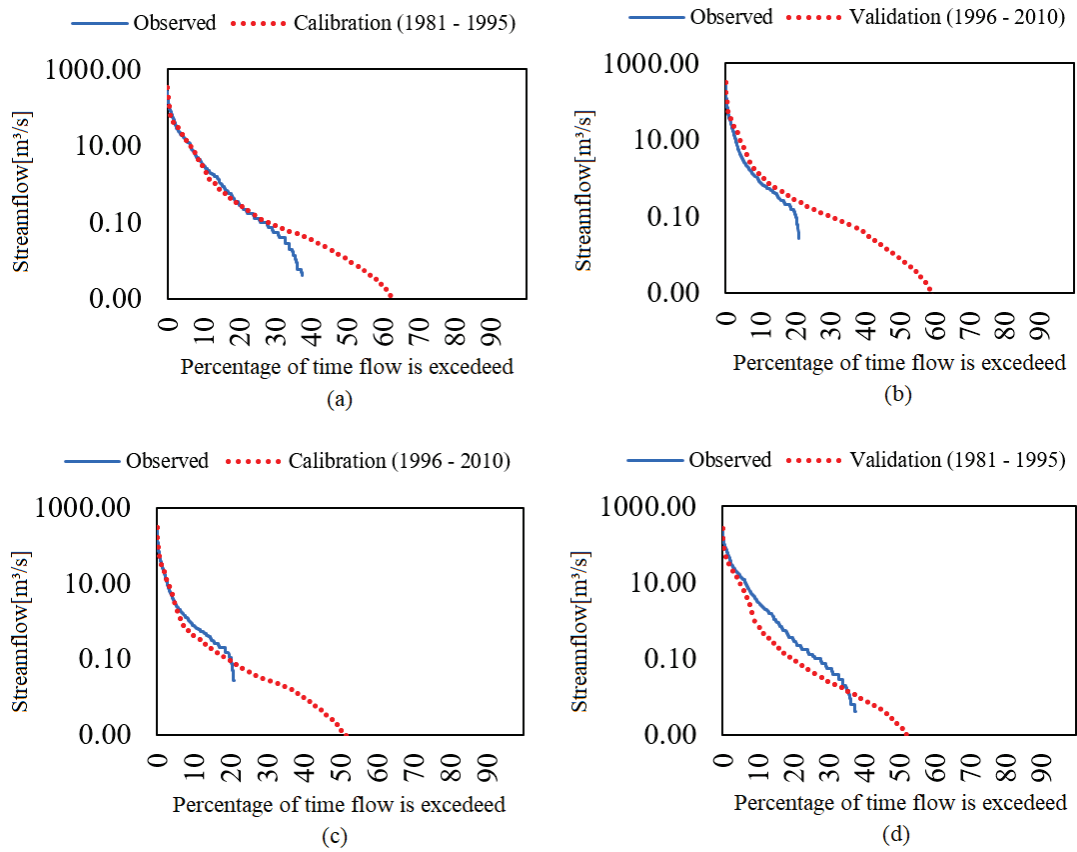


Figure 6 Comparison of observed and simulated log flow duration curves for: (a) calibration in 1981 – 1995; (b) validation in 1986 – 2010; (c) calibration in 1986 – 2010; (d) validation in 1981 – 1995.

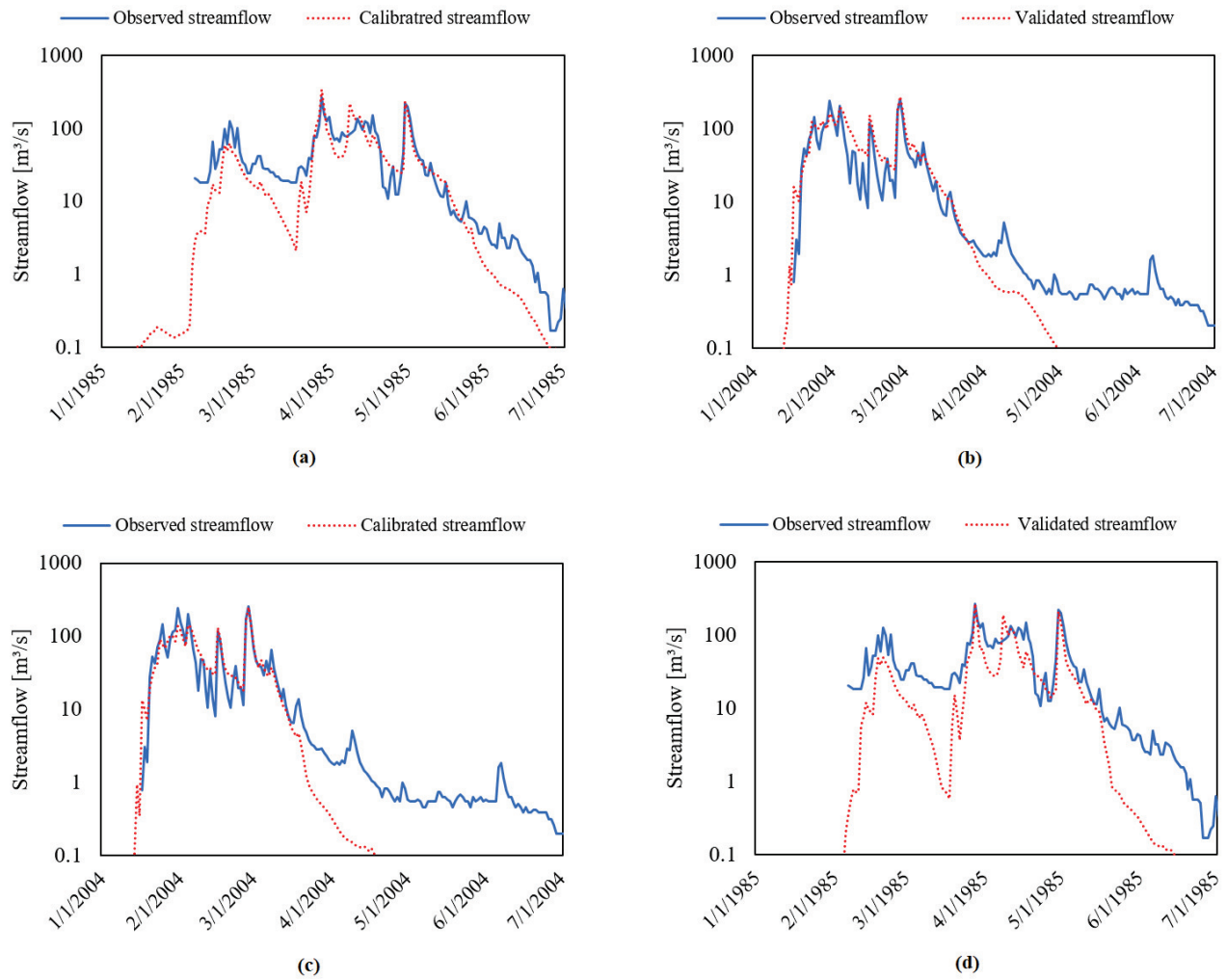
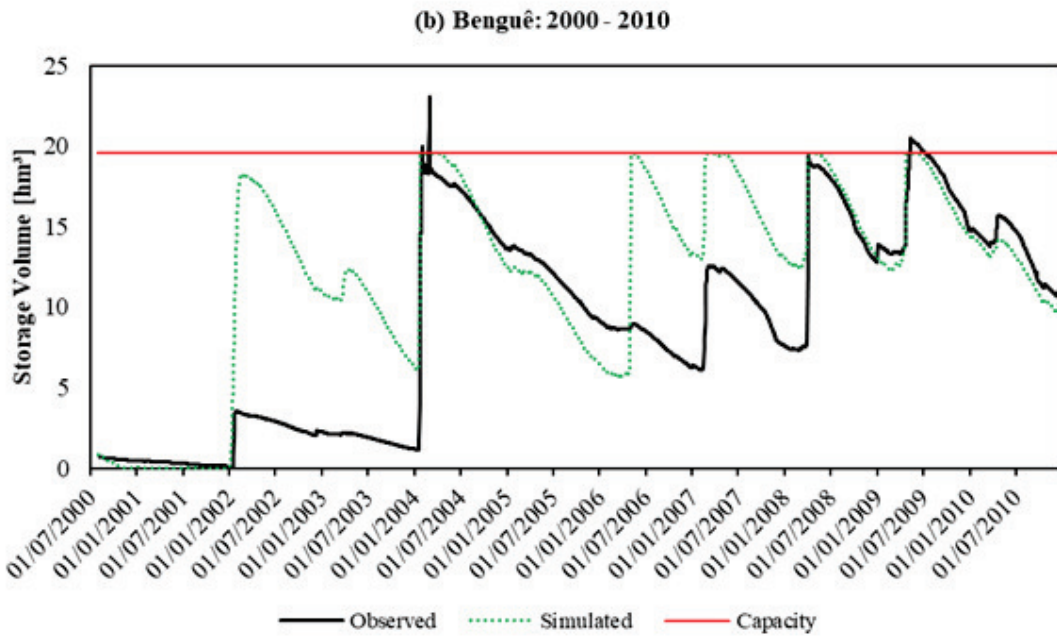
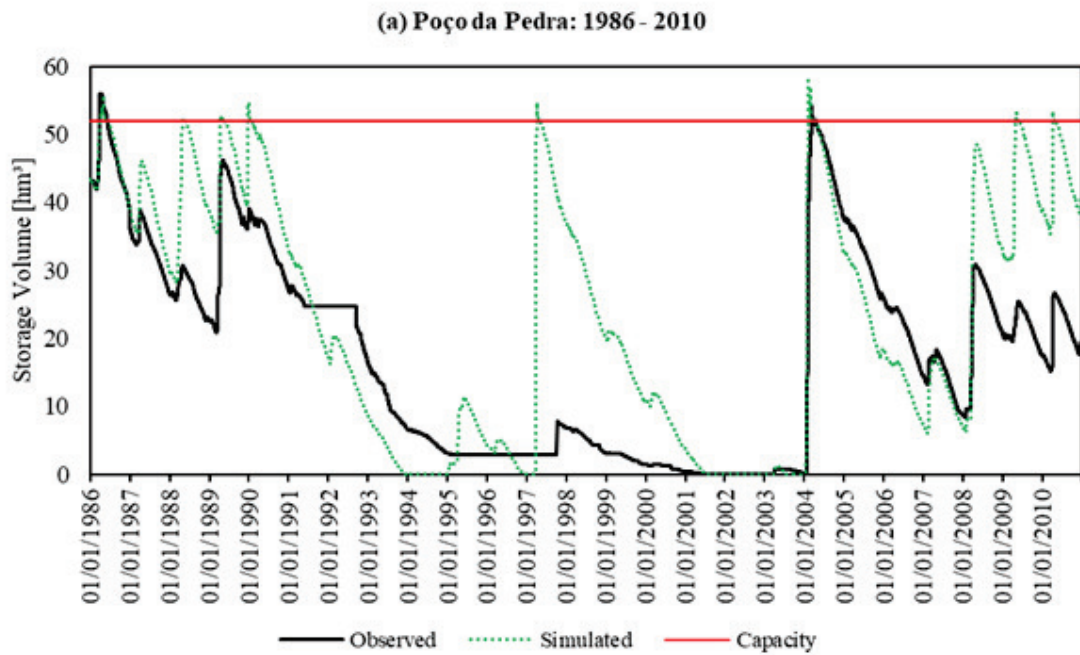


Figure 7 Comparison of observed and simulated hydrograph for daily discharges at Malhada gauging station for: (a) calibration year of 1985; (b) validation year of 2004; (c) calibration year of 2004; (d) validation year of 1985.



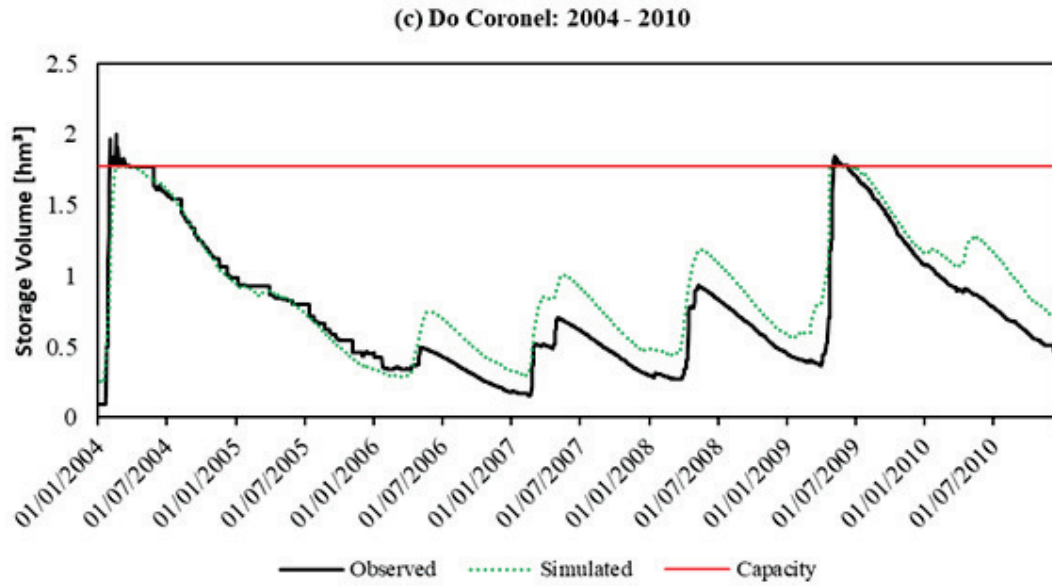
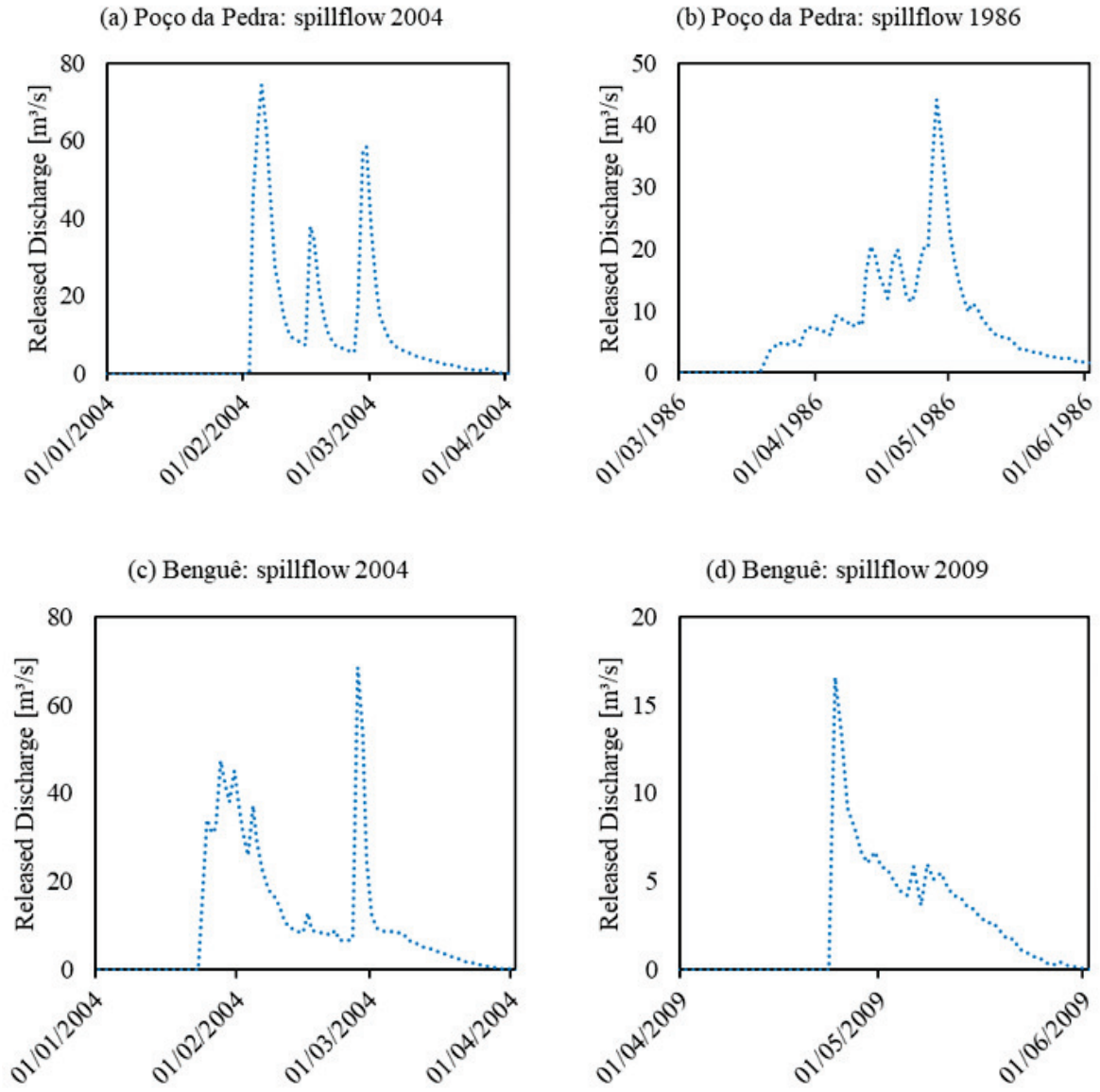


Figure 8 Comparison of observed by state water agency and simulated by SWAT daily storage volumes in the three strategic reservoirs for the calibration and validation periods: (a) Poço da Pedra (storage capacity 52 hm³, simulation 1986 - 2010) (b) Benguê (storage capacity 19.56 hm³, simulation 2000 - 2010), (c) Do Coronel (storage capacity 1.77 hm³, simulation 2004 - 2010).



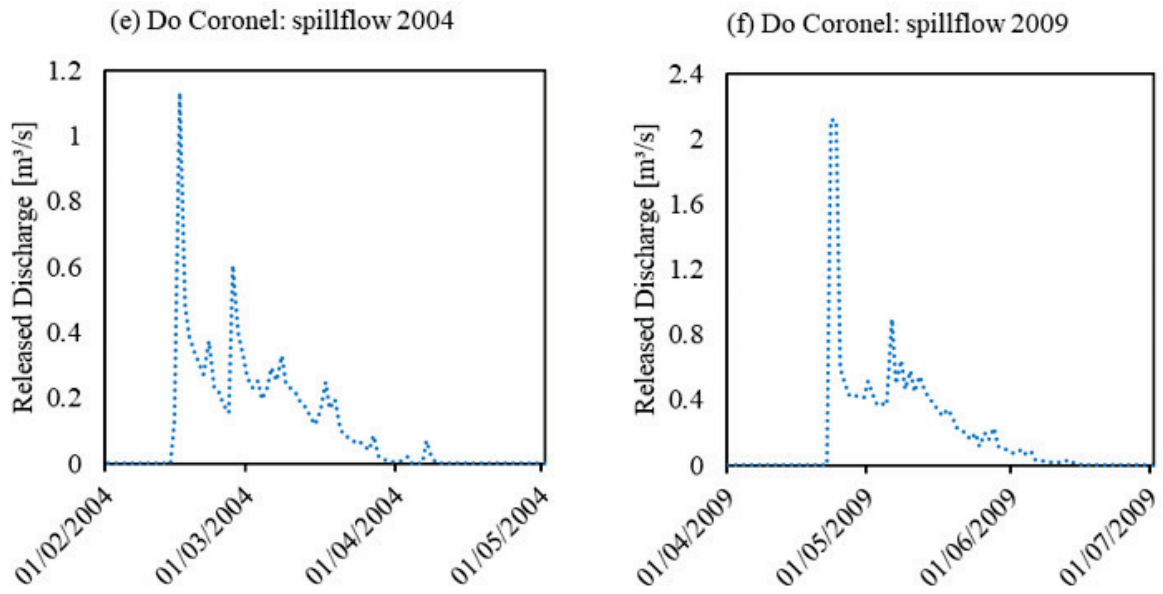


Figure 9 Hydrographs of released discharge for simulated outflow over the spillway of the three strategic reservoirs for model simulations: (a) Poço da Pedra – 2004; (b) Poço da Pedra – 1986; (c) Benguê – 2004; (d) Benguê – 2009; (e) Do Coronel – 2004; (f) Do Coronel – 2009.

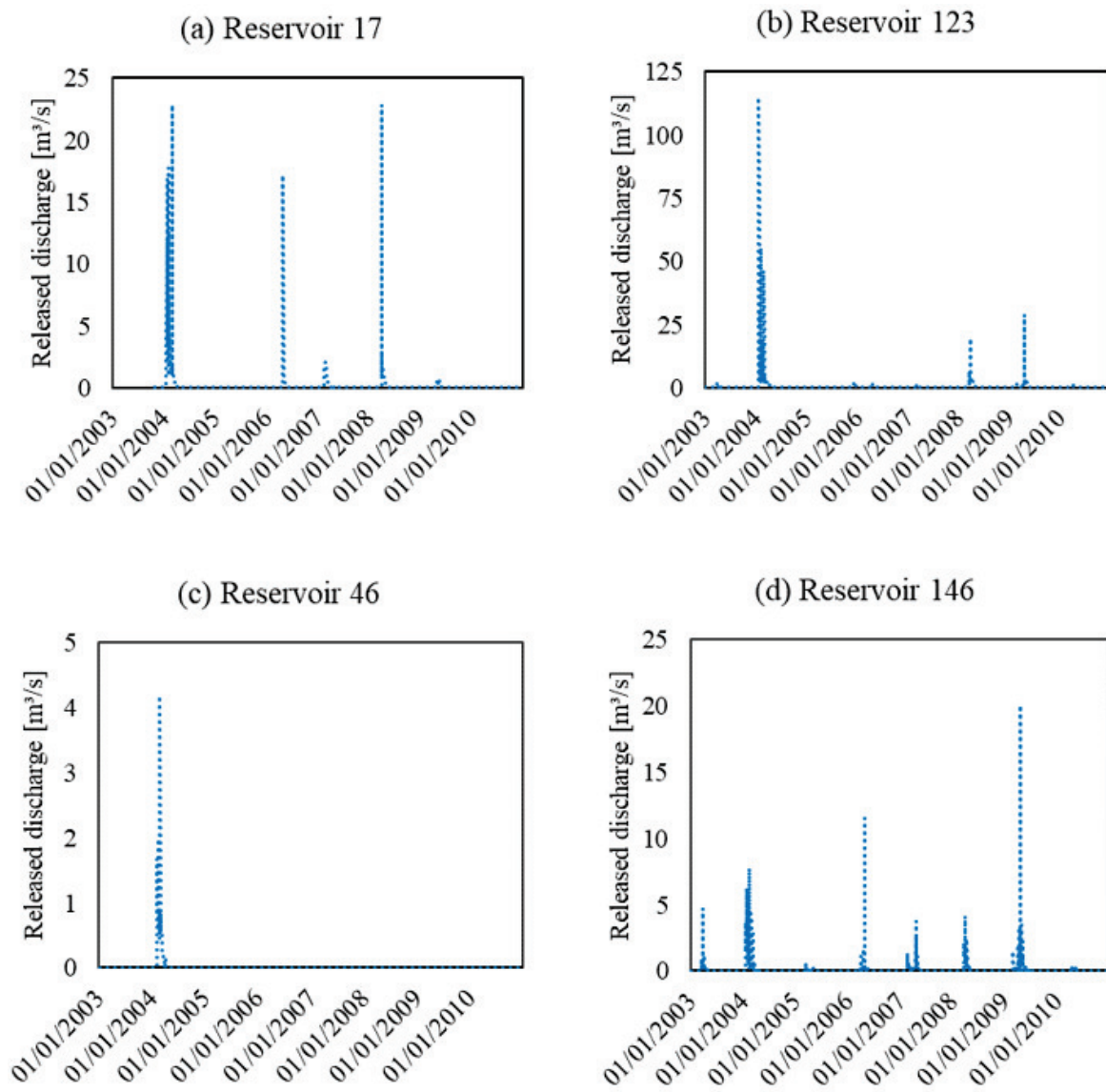


Figure 10 Hydrographs for simulated daily discharges released from the private reservoirs No. 17 (a), No. 123 (b), No. 46 (c) and No. 146 (d) via spillway for the years 2003-2010.

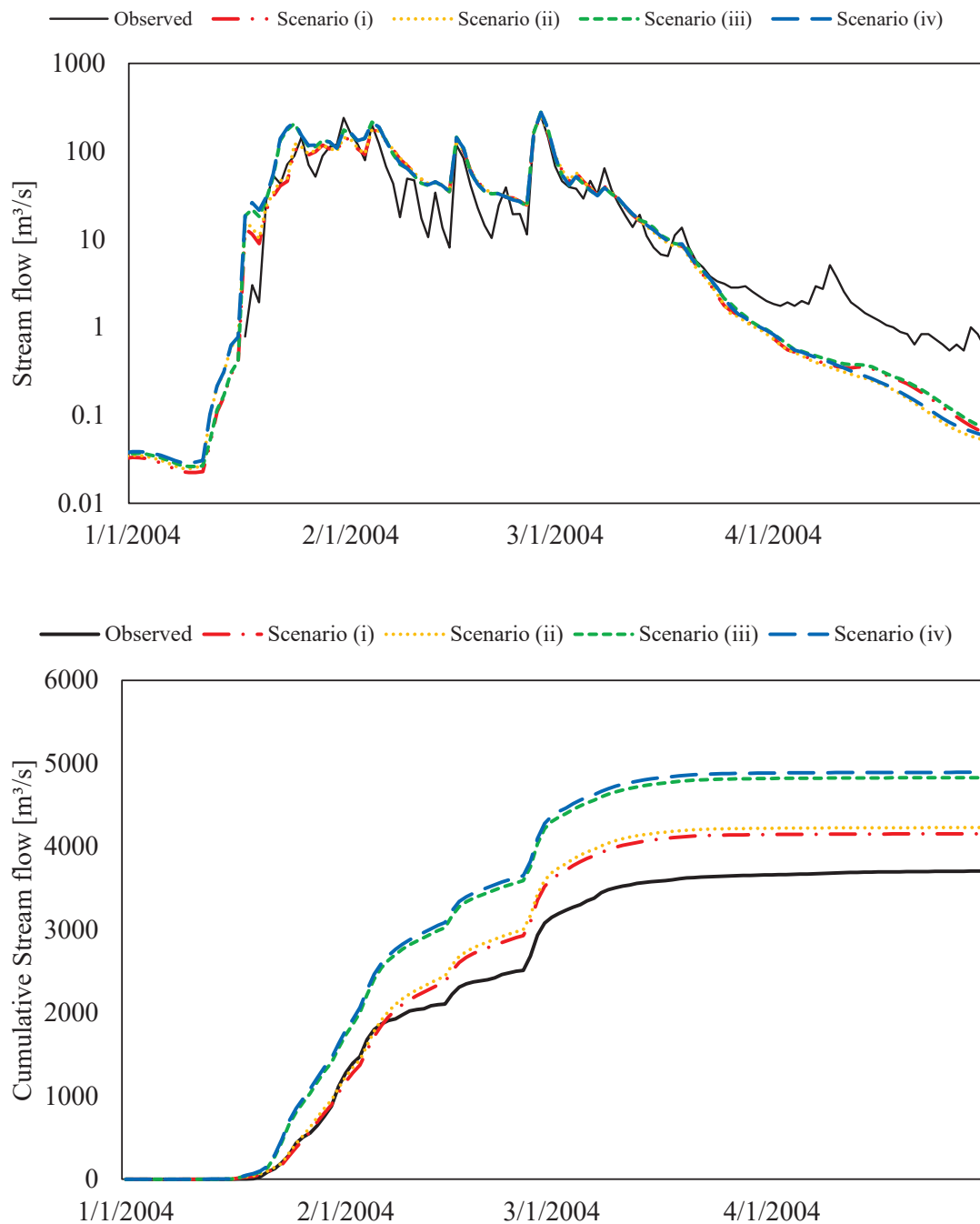


Figure 11 Hydrographs and cumulative stream flow at Malhada station showing observed values and 4 scenarios of reservoirs during the year of 2004: scenario (i) considering all strategic reservoirs and small reservoirs (reference); (ii) removing all small reservoirs in the hydrological system, but keeping only the strategic reservoirs; (iii) removing all strategic reservoirs but keeping only the small reservoirs; (iv) removing all reservoirs.

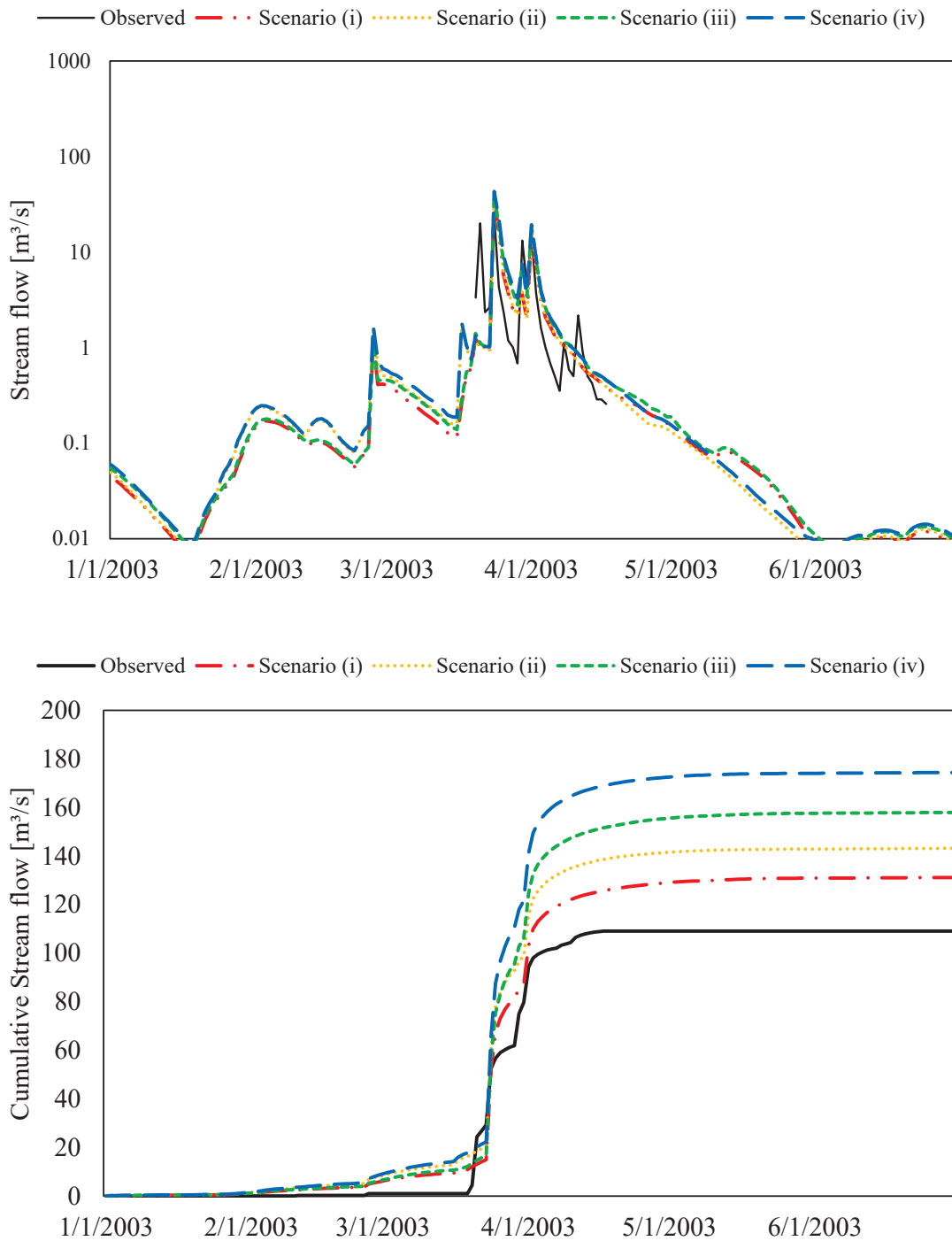


Figure 12 Hydrographs and cumulative stream flow at Malhada station showing observed values and 4 scenarios of reservoirs during the year of 2003: scenario (i) considering all strategic reservoirs and small reservoirs (reference); (ii) removing all small reservoirs in the hydrological system, but keeping only the strategic reservoirs; (iii) removing all strategic reservoirs but keeping only the small reservoirs; (iv) removing all reservoirs.

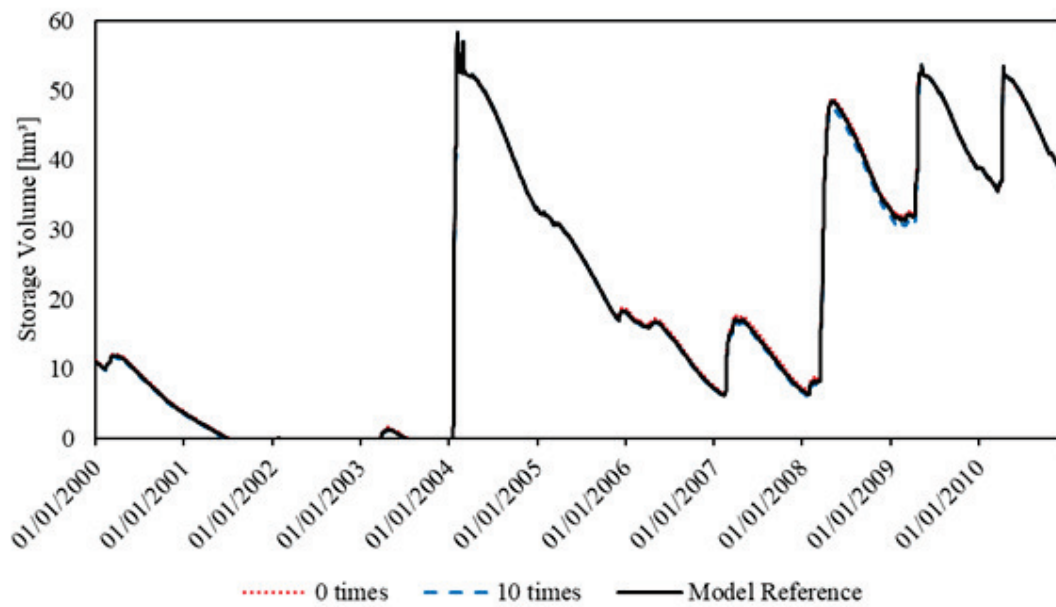


Figure 13 Comparison for storage volumes in Poço da Pedra (2000 – 2010) with modifications in the dimensions of the small reservoirs in 0 and 10 times. “0 times” means the total absence of small reservoirs. “10 times” means a ten times increase in the parameters that represent the volumes of these small reservoirs. Model reference means the original parameterization.

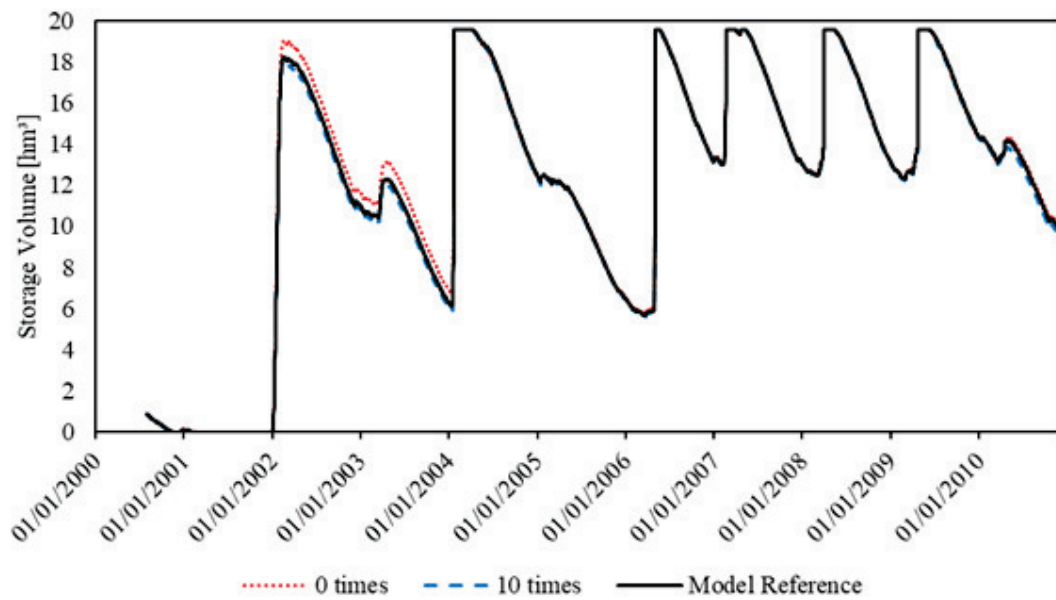


Figure 14 Comparison for storage volumes in Benguê (2000 – 2010) with modifications in the dimensions of the small reservoirs in 0 and 10 times. “0 times” means the total absence of small reservoirs. “10 times” means a ten times increase in the parameters that represent the volumes of these small reservoirs. Model reference means the original parameterization.

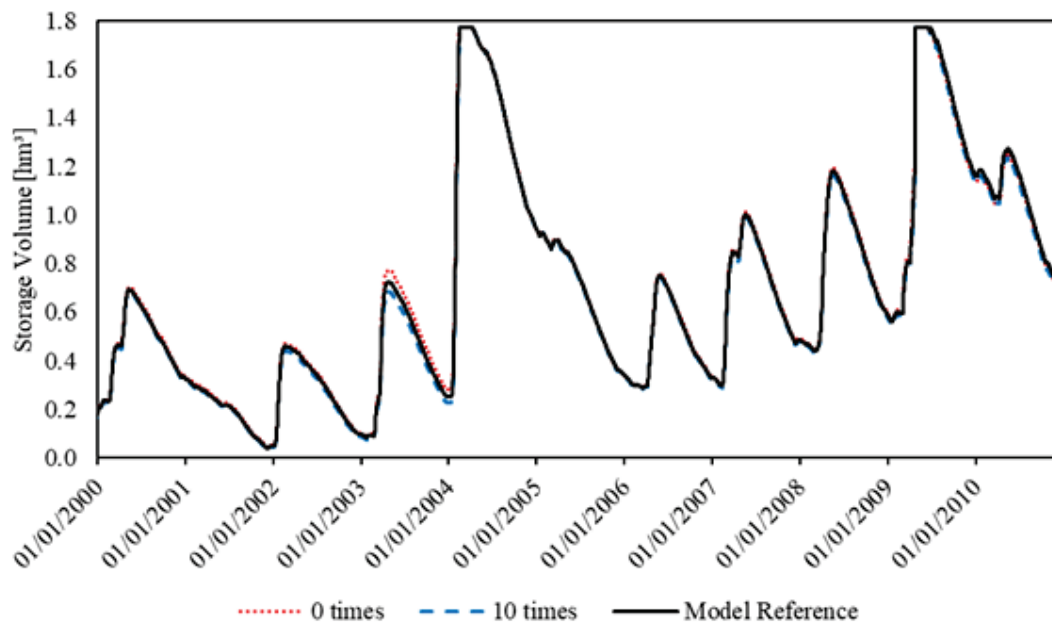


Figure 15 Comparison for storage volumes in Do Coronel (2000 – 2010) with modifications in the dimensions of the small reservoirs in 0 and 10 times. “0 times” means the total absence of small reservoirs. “10 times” means a ten times increase in the parameters that represent the volumes of these small reservoirs. Model reference means the original parameterization.

Table 1 Hydraulic structure of strategic reservoirs located in the study catchment. Data source: Secretary of Water Resources of the government of Ceará (SRH).

Item	Dam			
	Poço da Pedra	Do Coronel	Benguê	Mamoeiro
Operation year	1958	1946	2000	2012
Capacity [hm ³]	52.00	1.77	19.56	20.68
Flooded area at cap. [km ²]	8.320	0.5	3.479	3.691
Spillway type	n. i.	Concrete Sill	Type Creager	Type Creager
Spillway width (constant)	60	24	150	80
Height of spillway crest	22	13	18.54	18
Controllable outlet	yes	no	yes	yes

Table 2 Parameterization of reservoirs (water impoundments implemented into the model as reservoirs). Reservoir numbers and sub-basin numbers correspond to the IDs given automatically in

ArcGIS. Abbreviations B., dC., PP. and M. stand for Bengué, Do Coronel, Poço da Pedra and Mamoeiro, respectively

SWAT parameter	MORES	IYRES	RES_ESA	RES_EVOL	RES_PSA	RES_PVOL	RES_VOL	RES_K	EVRSV	IRESKO	RES_TARG	NDTARGR
Explanation	Month, in which reservoir became operational	Year, in which reservoir became operational	Surface area when reservoir filled to emergency spillway	Storage volume when reservoir filled to emergency spillway	Surface area when reservoir filled to principle spillway	Storage volume when reservoir filled to principle spillway	Initial reservoir storage volume	Hydraulic conductivity of reservoir bottom	Lake evaporation coefficient	Reservoir outflow simulation code	Manually set target volume (equal for each months)	No. of days to reach target storage from current reservoir storage
Res-No.	SB-No.											
2 (B.)	8	2000	438.00	2937.00	348.00	1956.00	85.80	0.0	1	2	1956.00	1.04
1 (dC.)	1	1979	100.00	300.00	50.00	177.00	46.80	0.0	1	2	177.00	1.08
0 (PP.)	11	1979	1639.00	14696.00	832.00	5200.00	1698.00	0.0	1	2	5200.00	2.25
174 (M.)	1	2012	454.00	2887.85	369.10	2068.30	82.73	0.0	1	2	2068.30	1.00
13	11	1994	22.56	66.91	15.89	38.19	0.00	0.1	1	2	38.19	1.01
17	11	2003	40.10	107.62	26.89	57.67	0.00	0.1	1	2	57.67	1.00
19	11	1999	23.13	63.44	15.77	34.66	0.00	0.1	1	2	34.66	1.00
24	1	1991	7.47	13.66	4.08	5.07	0.00	0.1	1	2	5.07	1.00
30	1	1979	21.93	62.36	15.17	34.66	3.47	0.1	1	2	34.66	1.00
32	1	1979	12.39	32.56	8.31	17.10	1.71	0.1	1	2	17.10	1.00
34	1	1979	10.96	24.59	6.82	11.34	1.13	0.1	1	2	11.34	1.00
46	1	1979	89.26	307.50	64.40	192.83	38.57	0.1	1	2	192.83	1.14
90	1	1979	14.75	37.03	9.71	18.78	1.88	0.1	1	2	18.78	1.00
123	1	1979	20.74	64.12	14.82	37.55	3.75	0.1	1	2	37.55	1.00
128	1	1979	4.19	12.91	2.97	7.56	0.00	0.1	1	2	7.56	1.00
146	1	1979	45.03	127.57	30.74	71.06	7.11	0.1	1	2	71.06	1.05
197	1	1979	8.91	18.15	5.25	7.60	0.00	0.1	1	2	7.60	1.00
203	1	1979	5.97	8.26	2.39	2.15	0.00	0.1	1	2	2.15	1.00

Table 3 Parameterization of ponds (water impoundments implemented into the model as ponds). Sub-basin numbers correspond to the IDs given automatically in ArcGIS.

SB No.	Drainage Fraction	Volume Principle (Vpr)	Surface Area Principle (SApr)	Volume Emergency (Vem)	Surface Area Emergency (SAem)	Initial Storage	NDTARG
	[-]	[10000 m ³]	[10000 m ²]	[10000 m ³]	[10000 m ²]	[10000 m ³]	[d]
2	0.1407	7.5238	8.6954	19.8279	16.2424	0	1
3	1	180.773	57.3379	245.2304	71.9404	36	1.35
5	0.4696	0.8167	1.8449	4.2163	5.1859	0	1
6	1	7.5132	9.6866	24.3122	23.3748	0	1
8	0.0391	3.7472	4.8147	10.7188	9.3316	0	1.23
10	0.4067	4.9495	7.3037	13.0763	15.9801	0	1
13	1	5.1694	5.8958	13.3848	10.7323	0	1
19	0.1458	0.8939	2.2837	5.4764	7.2734	0	1
23	0.0763	0.9053	1.9686	4.4619	5.374	0	1
25	1	1.2363	3.0887	7.26	9.4324	0	1
27	1	1.3203	2.4965	5.5348	6.1549	0	1
28	0.6053	1.5654	3.311	7.7935	9.624	0	1
33	1	0.3281	1.0389	2.6666	3.8864	0	1
34	0.3461	1.0677	2.184	4.8947	5.6966	0	1
36	0.2796	2.7783	3.9881	8.7843	8.2325	0	1
40	0.2456	0.2206	0.8092	2.2375	3.4799	0	1
43	1	2.3644	3.6029	7.9147	7.7095	0	1
46	0.8	0.6155	1.2528	3.2769	4.3561	0	1
59	0.8349	1.3593	3.6802	9.2813	12.9686	0	1
60	0.1041	0.1517	0.6393	1.9212	3.1614	0	1
61	1	5.4467	7.7014	17.1033	16.0336	0	1
64	0.3512	13.3103	10.6946	26.894	16.6532	1.3	1
65	1	5.1583	6.819	15.6876	14.6899	0	1
69	1	1.5008	4.0274	9.7324	13.1594	0	1
71	0.3748	1.1897	2.5641	6.0043	7.4319	0	1
72	0.819	1.7086	3.3212	7.5068	8.6277	0	1
74	0.4773	2.6592	4.4424	10.284	9.7641	0	1.22
75	0.0524	0.2017	0.8205	2.4195	3.9328	0	1
77	0.3162	2.9359	5.4036	12.6029	14.5969	0	1
79	0.2002	0.8926	2.127	4.9608	6.3172	0	1.02
80	0.4298	0.2251	1.0437	3.4006	5.8433	0	1
81	0.8215	0.6982	1.7436	4.1308	5.3995	0	1
82	0.7291	0.4968	1.5373	4.1508	6.2157	0	1
85	1	3.6826	4.7623	10.5934	9.2627	0	1
87	0.4025	2.9633	5.2069	11.8974	13.1948	0	1.05
88	0.95	0.7407	1.8059	4.2567	5.5043	0	1
90	1	1.5455	3.1587	7.5267	9.2915	0	1
93	1	7.5586	8.8378	20.4257	17.3195	0	1.02
95	0.7517	0.6823	1.6475	3.829	4.8805	0	1
98	0.4006	1.031	2.8662	7.3597	10.478	0	1
99	0.1782	0.7418	2.1364	5.2665	7.3392	0	1

SB No.	Drainage Fraction	Volume Principle (Vpr)	Surface Area Principle (SApr)	Volume Emergency (Vem)	Surface Area Emergency (SAem)	Initial Storage	NDTARG
	[-]	[10000 m ³]	[10000 m ²]	[10000 m ³]	[10000 m ²]	[10000 m ³]	[d]
100	1	29.5171	26.1075	64.7025	45.078	2.95	1.02
102	1	5.2178	7.5602	16.7197	15.8657	0	1
106	1	4.6885	5.7291	12.9448	11.0297	0	1
107	1	16.1602	13.5462	34.7797	24.2638	0	1
110	0.6358	6.8338	7.2609	17.1445	13.7023	0	1.04
112	0.0922	0.3418	1.066	2.7175	3.9329	0	1
113	0.3669	2.3219	5.0349	11.6349	14.25	0	1
117	0.081	4.1549	5.797	12.799	11.7793	0	1
119	0.1587	2.3743	4.6125	10.3382	11.7731	0	1
120	1	6.3861	8.8767	19.733	18.2893	0	1.05
122	1	3.6661	6.3311	14.2447	15.3917	0	1
123	1	4.1293	6.2352	14.076	14.1237	0	1
124	0.9464	2.5164	4.4371	10.3236	11.7177	0	1
128	0.1765	0.3815	1.1425	2.8614	4.0627	0	1
131	0.1025	0.578	1.4841	3.5123	4.6224	0	1
132	0.191	2.0321	4.3421	9.9109	11.9397	0	1
134	1	9.3236	13.8683	31.2845	31.0957	0	1
135	1	31.3789	22.0259	59.2537	34.1384	3.14	1.02
137	0.2512	1.0437	2.5996	6.1387	7.9998	0	1
138	0.1997	0.4126	1.2002	2.9704	4.1595	0	1
139	1	3.279	4.4266	9.7989	8.819	0	1
142	1	3.8062	5.6076	12.4575	12.0347	0	1
144	0.9	0.7818	1.7949	4.1178	5.1092	0	1
149	0.2237	0.1046	0.5058	1.6715	2.8961	0	1
150	0.5671	0.3025	0.9872	2.5698	3.7969	0	1
153	0.1916	25.1365	15.9595	44.4581	22.853	2.51	1.15
154	0.0536	0.0951	0.4765	1.6162	2.8355	0	1
157	0.1087	0.6223	1.8313	4.6474	6.6331	0	1.05
159	1	0.304	0.9902	2.5753	3.802	0	1
168	0.3333	0.7133	1.6942	3.9201	4.9533	0	1.19
171	0.9508	3.1478	4.3143	9.5366	8.6696	0	1
173	0.1667	0.2131	0.7918	2.2051	3.4481	0	1
175	1	2.5427	3.7716	8.2931	7.9395	0	1
181	1	2.6293	3.852	8.4747	8.0486	0	1
183	0.0633	5.2966	5.9868	13.6159	10.8486	0	1.07
187	0.0855	0.3322	1.0472	2.6822	3.9006	0	1
193	1	2.8781	4.0776	8.9893	8.3529	0	1
195	1	1.0286	2.1333	4.7922	5.6212	0	1

Table 4 Parameterization of calibrated model: Parameters set for the entire catchment.

Entire Catchment	
Calibrated Parameters	Calibrated Value
GW_DELAY	12 d and 30 d
CH_K1	5 mm/h to 72 mm/h
TRNSRCH	0.3
OV_N	0.6
CN2	57.34 to 92
CH_N1	0.065
CANMX	1.5

Table 5 Parameterization of calibrated model: Parameters set for specific sub-basins of the catchment. Distinction between sub-catchments of two strategic reservoirs and topographic position of sub-basins.

Item of Distinction	Sub-catchments		Specific Sub-basins			
Calibrated Parameters	Poço da Pedra Catchment	Benguê Catchment	Upstream SB	Transition SB/Medium-order Reaches	Downstream SB/High-order Reaches	Lowlands (incl. Do Coronel Sub-catchment)
	Calibrated Values					
REVAPMN	265	265	265	265	265	265
GW_REVAP	0.15	0.15	0.25	0.15	0.1	0.25
GWQMN	700	700	700	700	700	700
CH_K2	25	19	5	20	72	72
CH_N2	0.05	0.05	0.05	0.05	0.05	0.05
SURLAG	4	4	4	4	4	4
ALPHA_BF	0.8	0.8	0.8	0.8	0.8	0.8
RCHARG_DP	0.25	0.25	0.25	0.25	0.25	0.25
ALPHA_BNK	0.6	0.6	0.6	0.6	0.6	0.6

Table 6 Parameterization of calibrated model: Parameters set for specific zones in the catchment. Distinction between soil types.

Item of Distinction	Soil Type				
	Bruno	Latosol	LitolicosEu	Planosolos	Podisolico-EqEu
	Calibrated Values				
ESCO	0.02	0.02	0.02	0.02	0.02
LAT_TTIME	0	0	0	0	0
SOL_K	PTF results	PTF results	PTF results x 0.8	PTF results	PTF results
SOL_AWC	PTF results	PTF results	PTF results x 1.2	PTF results	PTF results
GW_REVAP	0.1 and 0.15	0.15	0.1, 0.15 and 0.25	0.25	0.1 and 0.15
SOL_CRK	0.3	0.4	0.3	0.01	0.01

Table 7 Evaluation of model performance in streamflow at Malhada gauging station with statistical methods for calibration period in 2-fold cross-validation of the series, where PBIAS is the percent bias, NSE is the Nash-Sutcliffe Efficiency and KGE is the Kling-Gupta Efficiency.

Performance criterion	Calibration Value (1981 – 1995)	Validation Value (1996 – 2010)	Calibration Value (1996 – 2010)	Validation Value (1981 – 1995)
PBIAS (%)	5.22	-38.93	2.29	33.55
NSE	0.65	0.56	0.65	0.65
KGE	0.81	0.53	0.82	0.55

Table 8 Comparison between the number of days with spillway outflow for observed data and the number of days with spillway outflow for model simulations during periods with data availability for reservoirs: 1986 - 2010 for Poço da Pedra, 2000 - 2010 for Benguê and 1998 - 2010 for Do Coronel.

Reservoir	Number of days with spillway outflow observed	Number of days with spillway outflow simulated
Poço da Pedra	97	316
Benguê	64	231
Do Coronel	93	110

Table 9 Comparison of model results in streamflow at Malhada gauging station for different reservoir scenarios (1979 - 2010).

Performance criterion	Scenario (i) (reference)	Scenario (ii) (only strategic reservoirs)	Scenario (iii) (only small reservoirs)	Scenario (iv) (no reservoirs)
PBIAS (%)	0.53	-2.76	-16.99	-20.30
NSE	0.63	0.61	0.51	0.48
KGE	0.81	0.80	0.70	0.66